statistically significant. All values are expressed as mean ± standard error of the mean (S.E.M., n = number).

2.13. *Ethical considerations*

All studies were performed in the laboratories of the Department of Diabetes and Clinical Nutrition, Kyoto University, in accordance with the Declaration of Helsinki. The Animal Care Committee of Kyoto University Graduate School of Medicine approved animal care and procedures.

3. Results

3.1. *Effect of CRA on gluconeogenesis from lactate in rat liver perfusion*

The effect of CRA on gluconeogenesis was investigated in rat liver perfusion. Glucose output into the effluent perfusate was stabilized under 2 μmol/g/h. Upon changing perfusate from basal buffer to KRB containing 2 mM lactate, the glucose output rate increased rapidly and reached a steady state of approximately 10 μmol/g/h (Fig. 2). Glucose output rate was reduced by the addition of 100 μM CRA to the buffer, and continued to fall during the 20 min perfusion with CRA. After 100 μM CRA perfusion, the glucose output rate was 7.3 ± 0.3 μmol/g liver/h, approximately 73% of that before CRA perfusion. Glucose output gradually recovered after washout of CRA with glucose-free KRB containing 2 mM lactate, and, after washout of lactate, fell to under 2 μmol/g/h. Average glucose output rate during the last 14 min of the 20 min perfusion (66–80 min) with KRB containing 20–100 μM CRA was then measured and compared to control (Fig. 3). The glucose output was significantly

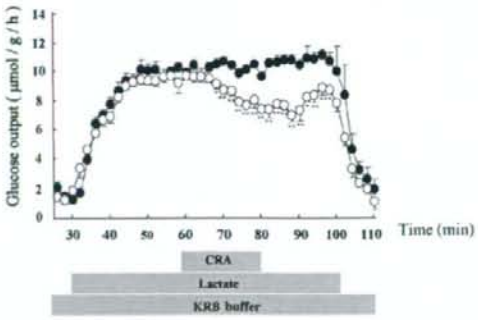

Fig. 2 – Inhibitory effect of CRA on glucose output rate in perfused rat liver. Liver was perfused with glucose-free KRB buffer for 110 min, and from 30 to 100 min with glucose-free buffer containing 2 mM lactate. From 60 to 80 min, perfusion was with buffer containing 2 mM lactate and with 100 μM CRA. From 100 to 110 min, perfusion was with glucose-free KRB buffer without lactate. Effluent perfusate was collected every 2 min, and glucose content was measured. CRA (○), control (●). Data are shown as means with S.E.M. (n = 5 for each group). *$P < 0.05$, **$P < 0.01$ compared with the value of control.

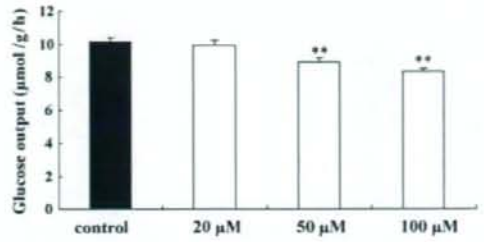

Fig. 3 – Effect of CRA on glucose output rate in perfused rat liver. Liver was perfused as in Fig. 2. Average glucose output rate during the last 14 min (66–80 min) perfusion period with buffer containing 20–100 μM CRA was compared. CRA (□), control (■). Data are shown as means with S.E.M. (n = 5 for each group). **$P < 0.01$ compared with the value of control.

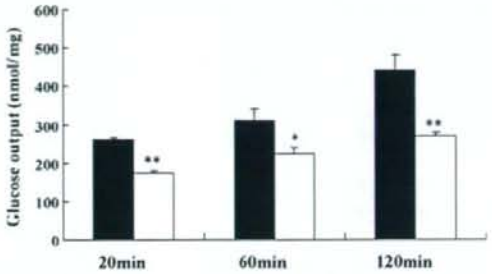

Fig. 4 – Time course of the inhibitory effect of CRA on gluconeogenesis in isolated hepatocytes. Hepatocytes were incubated at 37 °C in a humidified atmosphere (5% CO_2) of DMEM without glucose but containing 1 mM lactate and 0.24 mM IBMX in the presence of 100 μM CRA or vehicle for 20, 60, and 120 min. Glucose content in supernatant was measured by glucose oxidation method. CRA (□), control (■). Data are shown as means with S.E.M. (n = 8 for each group). *$P < 0.05$, **$P < 0.01$ compared with the value of control.

reduced by the addition of 50 μM (12%) and 100 μM (18%) of CRA compared to control ($P < 0.01$), dose-dependently in the 20–100 μM CRA range.

3.2. *Effect of CRA on gluconeogenesis from lactate in isolated hepatocytes*

The effect of CRA on gluconeogenesis from lactate was investigated in hepatocytes. Fig. 4 shows the time course of inhibition by CRA of hepatic gluconeogenesis from lactate. The gluconeogenesis from lactate increased in a time-dependent manner linearly up to 120 min, indicating that the metabolic flow in the hepatocytes was at a steady state both in the presence and in the absence of CRA. After 20, 60, and 120 min exposure to 100 μM CRA, hepatic gluconeogenesis was significantly inhibited compared to control. The gluconeogenesis

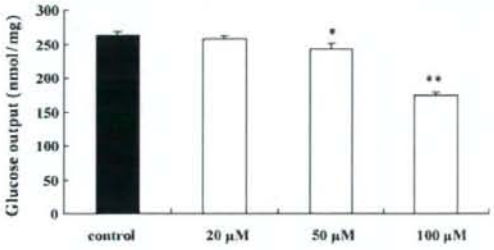

Fig. 5 – Concentration-dependence of the inhibitory effect of CRA on gluconeogenesis in isolated hepatocytes. Hepatocytes were incubated at 37 °C in a humidified atmosphere (5% CO_2) of DMEM without glucose but containing 1 mM lactate and 0.24 mM IBMX in the presence of 20–100 μM CRA or vehicle for 20 min. Glucose content in supernatant was measured by glucose oxidation method. CRA (□), control (■). Data are shown as means with S.E.M. ($n = 9$ for each group). *$P < 0.05$, **$P < 0.01$ compared with the value of control.

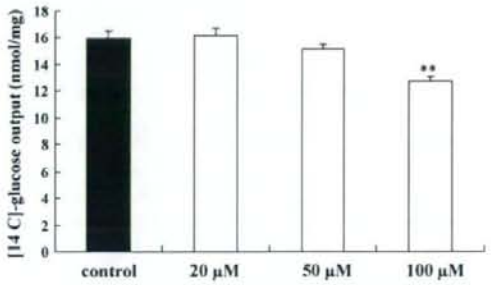

Fig. 7 – Concentration dependence of the inhibitory effect of CRA on neosynthesized [^{14}C]-glucose in isolated hepatocytes. Hepatocytes were incubated at 37 °C in a humidified atmosphere (5% CO_2) in DMEM with 10 mM glucose, 1 mM pyruvate and 0.24 mM IBMX, and 0.05 μCi of [^{14}C]-pyruvate in the presence of 20–100 μM CRA or vehicle for 20 min. Radioactivity was measured by liquid scintillation counting. CRA (□), control (■). Data are shown as means with S.E.M. ($n = 4$ for each group). **$P < 0.01$ compared with the value of control.

in hepatocytes decreased in a dose-dependent manner after 20 min incubation with CRA (Fig. 5).

3.3. *Effect of CRA on neosynthesized [^{14}C]-glucose in isolated hepatocytes*

The effect of CRA on gluconeogenesis from [^{14}C]-pyruvate in the presence of 10 mM glucose in culture medium was investigated in isolated hepatocytes. Fig. 6 shows the time course of inhibition by CRA of hepatic gluconeogenesis from [^{14}C]-pyruvate. The gluconeogenesis from [^{14}C]-pyruvate increased in a time-dependent manner linearly up to 120 min, indicating that the metabolic flow in the hepatocytes was at a steady state both in the presence and in the absence of CRA. After 20, 60, and 120 min exposure to 100 μM CRA, hepatic gluconeogenesis was significantly inhibited compared to control. The gluconeogenesis from [^{14}C]-pyruvate decreased in a dose-dependent manner after 20 min incubation with CRA (Fig. 7). Thus, CRA inhibited hepatic gluconeogenesis in the presence of 10 mM glucose as well as in the absence of glucose in culture medium.

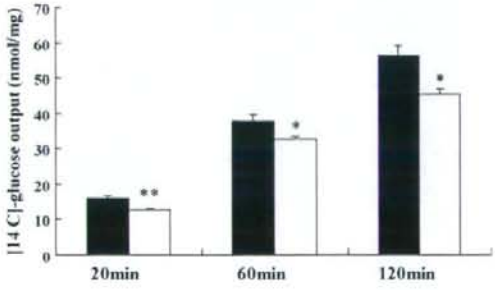

Fig. 6 – Time course of the inhibitory effect of CRA on neosynthesized [^{14}C]-glucose in isolated hepatocytes. Hepatocytes were incubated at 37 °C in a humidified atmosphere (5% CO_2) in DMEM with 10 mM glucose, 1 mM pyruvate and 0.24 mM IBMX, and 0.05 μCi of [^{14}C]-pyruvate in the presence of 100 μM CRA or vehicle for 20, 60, and 120 min. Radioactivity was measured by liquid scintillation counter. CRA (□), control (■). Data are shown as means with S.E.M. ($n = 4$ for each group). *$P < 0.05$, **$P < 0.01$ compared with the value of control.

3.4. *Effect of CRA on F-2,6-BP production in isolated hepatocytes*

The effect of CRA on the production of F-2,6-BP was examined in isolated hepatocytes. Hepatocytes were incubated in glucose-free medium with 100 μM CRA for 20 min, and the F-2,6-BP was then measured. CRA increased F-2,6-BP production in hepatocytes approximately 2-fold compared to control ($P < 0.05$) (Fig. 8). Next, hepatocytes were incubated in 10 mM glucose with 100 μM CRA for 20 min, and the F-2,6-BP was then measured. The addition of 10 mM glucose doubled the basal F-2,6-BP. In the presence of 10 mM glucose, CRA again increased F-2,6-BP production in hepatocytes approximately 1.5-fold compared to control, clearly indicating the central role of cellular F-2,6-BP levels in CRA inhibition of gluconeogenesis ($P < 0.01$) (Fig. 8).

3.5. *Effect of CRA on intracellular cAMP level in isolated hepatocytes*

To further clarify the mechanism of action of CRA, we compared the intracellular cAMP levels in isolated hepatocytes. CRA reduced the cAMP level in hepatocytes after incubation for 20 min ($P < 0.05$) (Fig. 9A). Forskolin, which activates the catalytic subunit of adenylate cyclase, evoked a

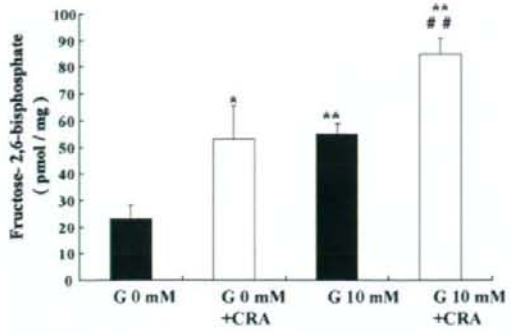

Fig. 8 – Effect of CRA on F-2,6-BP production in isolated hepatocytes. Hepatocytes were incubated at 37 °C in a humidified atmosphere (5% CO_2) in DMEM with or without 10 mM glucose (G) but containing 1 mM lactate and 0.24 mM IBMX in the presence of 100 μM CRA or vehicle for 20 min. CRA (□), control (■). Data are shown as means with S.E.M. (n = 5–7 for each group). *$P < 0.05$, **$P < 0.01$ compared to the value of control without glucose. ##$P < 0.01$ compared to the value control with 10 mM glucose.

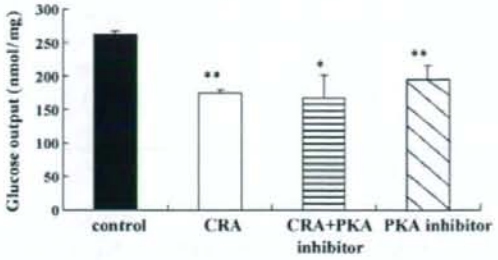

Fig. 10 – Effect of CRA on gluconeogenesis with a PKA inhibitor (H89) in isolated hepatocytes. Hepatocytes were incubated at 37 °C in a humidified atmosphere (5% CO_2) in DMEM without glucose but containing 1 mM lactate, 0.24 mM IBMX with/without 10 μM H89 in the presence of 100 μM CRA or vehicle for 20 min. Glucose content in supernatant was measured by glucose oxidation method. CRA (□), control (■), CRA + PKA inhibitor (▤), PKA inhibitor (▨). Data are shown as means with S.E.M. (n = 9 for each group). *$P < 0.05$, **$P < 0.01$ compared with the value of control.

marked elevation of the cAMP level after incubation for 20 min. CRA also reduced the forskolin-evoked increment of the cAMP level after incubation for 20 min ($P < 0.05$) (Fig. 9B).

3.6. *Effect of CRA on gluconeogenesis with cAMP-dependent protein kinase (PKA) inhibitor in isolated hepatocytes*

Hepatic gluconeogenesis in isolated hepatocytes was inhibited after 20 min exposure to the PKA inhibitor, N-[2-(*p*-bromocinnamylamino)ethyl]-5-isoquinolinesulfonamide (H89) at the concentration of 10 μM (Fig. 10). We also evaluated the effect of CRA on gluconeogenesis in hepatocytes in the presence of 10 μM H89. The PKA inhibitor did not have an additive inhibitory effect on CRA-induced inhibition of gluconeogenesis.

3.7. *Effects of CRA on GK activity and G6Pase activity in isolated hepatocytes*

The level of F-2,6-BP is regulated by the synthesizing (6-phosphofructo-2-kinase, PFK-2) and the degrading (fructose-2,6-bisphosphatase, F-2,6-BPase) enzyme complex. In insulin-producing cells, PFK-2/F-2,6-BPase reportedly interacts with GK, and the overexpression of PFK-2/F-2,6-BPase increases GK activity. In this study, CRA was found to increase the level of F-2,6-BP in isolated hepatocytes. Therefore, we measured GK activity after exposure to CRA. Hepatocytes were incubated with 100 μM CRA for 20 min, and GK activity was then measured. CRA significantly increased GK activity compared to control (control: 0.82 ± 0.04, n = 5, CRA: 1.09 ± 0.02 nmol/mg protein/min, n = 5; $P < 0.01$).

Since G6Pase is also a rate-limiting enzyme of gluconeogenesis, we measured G6Pase activity after exposure to CRA.

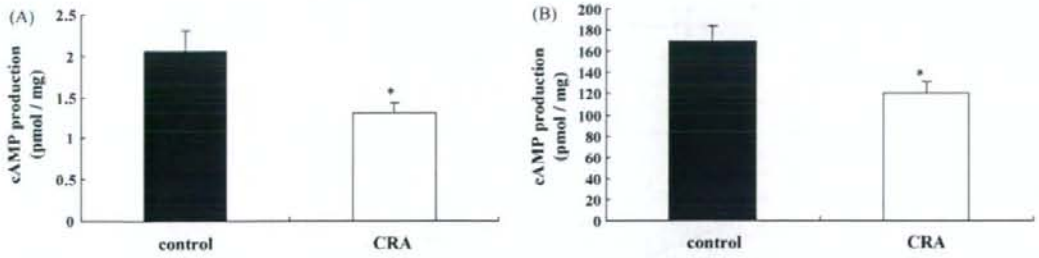

Fig. 9 – Effect of CRA on cAMP level in isolated hepatocytes. Hepatocytes were incubated at 37 °C in a humidified atmosphere (5% CO_2) in DMEM without glucose but containing 1 mM lactate and 0.24 mM IBMX without (A) or with (B) 5 μM forskolin in the presence of 100 μM CRA or vehicle for 20 min. CRA (□), control (■). Data are shown as means with S.E.M. (n = 4–6 for each group). *$P < 0.05$ compared with the value of control.

Hepatocytes were incubated with 100 μM CRA for 20 min, and G6Pase activity was then measured. CRA did not alter G6Pase activity (control: 140 ± 22, $n = 5$, CRA: 168 ± 37 nmol/mg protein/min, $n = 5$; $P = 0.55$).

4. Discussion

This is the first study to demonstrate that CRA reduces hepatic glucose production. We showed that CRA decreases gluconeogenesis in perfused rat liver in a dose-dependent manner (20–100 μM). We also showed that CRA decreases gluconeogenesis in isolated hepatocytes both in glucose-free medium and in glucose-containing medium in a dose-dependent manner (20–100 μM).

To determine whether the CRA concentration used in this study is physiologically relevant, we measured CRA in the blood after oral administration in dog. When CRA was orally administered at 20 mg/kg of body weight in dog, the concentration in peripheral blood was 17 μM after 90 min (unpublished data). In this study, CRA was found to inhibit hepatic gluconeogenesis at a concentration about 5-fold higher than that used in dog. Considering that the concentration of CRA in the portal vein should be higher than that in the peripheral vein when orally administered, the dosage of CRA used in these experiments seems appropriate.

To investigate the mechanism of action of CRA, we measured its effect on the production of F-2,6-BP, which plays an important role in the regulation of both glycolysis and gluconeogenesis. F-2,6-BP is a potent physiological activator of PFK-1, the rate-limiting enzyme in glycolysis [21,22], and inhibits fructose-1,6-bisphosphatase (F-1,6-BPase), an enzyme active in gluconeogenesis [23,24] (Fig. 11). In this study, CRA was found to markedly enhance the F-2,6-BP production during lactate-stimulated gluconeogenesis. Thus, CRA-induced increase in F-2,6-BP stimulates glycolysis and inhibits gluconeogenesis.

The activity of the synthesizing (PFK-2) and the degrading (F-2,6-BPase) enzyme of F-2,6-BP is determined by the phosphorylation state of PKA. Activation of PFK-2 is known to elevate cellular levels of F-2,6-BP, and cAMP inactivates PFK-2 activity through PKA in hepatocytes. On the other hand, cAMP activates F-2,6-BPase through PKA in hepatocytes [25]. In this study, we found that CRA decreases the cAMP level in isolated hepatocytes, suggesting that CRA increases F-2,6-BP by lowering intracellular cAMP level. We also found that a PKA inhibitor (H89) decreased gluconeogenesis in isolated hepatocytes, but did not have an additive inhibitory effect on CRA-induced inhibition of gluconeogenesis. Thus, CRA would seem to inhibit hepatic gluconeogenesis through the PKA-mediated pathway. However, CRA was found to reduce the forskolin-evoked increment of intracellular cAMP level. Thus, the mechanism by which CRA decreases the intracellular cAMP level must be investigated in further study.

Recently, Massa et al. [26] reported that PFK-2/F-2,6-BPase enzyme complex interacts with GK in the insulin-producing cells and that overexpression of PFK-2/F-2,6-BPase increases GK activity. In this study, we measured GK activity after exposure to CRA in isolated hepatocytes. CRA was found to increase GK activity, leading to glycolysis in the hepatocytes. On the other hand, Wen et al. [9] reported that CRA inhibited glycogen phospholylase *a* purified from rat liver. This direct effect of CRA on the enzyme of glycogen phospholylase suggests that CRA might inhibit glycogenolysis, another pathway to glucose production besides gluconeogenesis. Thus, the increased glycolysis and decreased glycogenolysis in hepatocytes may also contribute to the anti-diabetic action of CRA.

It was previously shown that Banaba leaf extract (1% CRA) decreases blood glucose levels in humans in a dose-dependent manner [27]. In addition, CRA has been shown to reduce post

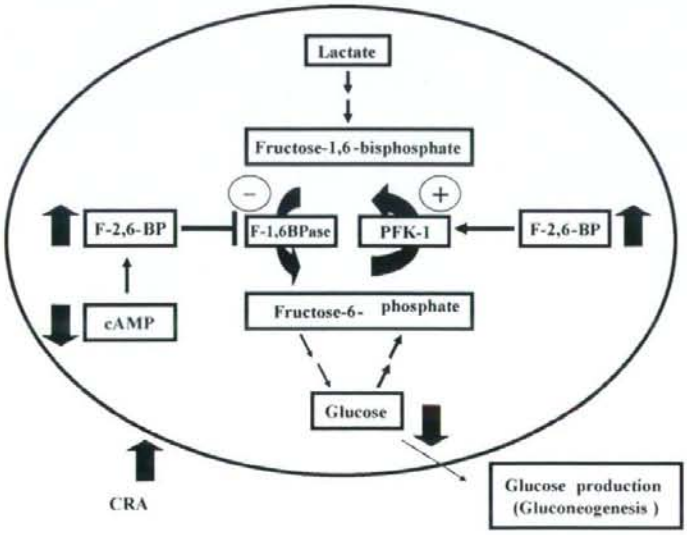

Fig. 11 – Mechanism of inhibitory action of CRA on gluconeogenesis.

challenge plasma glucose levels in human [11]. Considered together, these data suggest that CRA may provide a valuable new therapy in the treatment of type 2 diabetes.

Acknowledgments

This study was supported in part by Grants-in-Aids for Scientific Research from the Ministry of Education, Culture, Sports, Science and Technology of Japan; Health and Labour Sciences Research Grants for Research on Human Genome, Tissue Engineering, and Food Biotechnology from the Ministry of Health, Labor and Welfare of Japan; and Health and Labour Sciences Research Grants for Comprehensive Research on Aging and Health from the Ministry of Health, Labor and Welfare of Japan.

Conflict of interest

The authors state that they have no conflicts of interest.

REFERENCES

[1] E. Quisumbing, Medicinal Plants of the Phillippines, Katha Publishing, Quezon City, 1978, pp. 640–642.
[2] N. Banno, T. Akihisa, H. Tokuda, K. Yasukawa, H. Higashihara, M. Ukiya, et al., Triterpene acids from the leaves of Perilla frutescens and their anti-inflammatory and antitumor-promoting effects, Biosci. Biotechnol. Biochem. 68 (2004) 85–90.
[3] M. Yoshida, M. Fuchigami, T. Nagao, H. Okabe, K. Matsunaga, J. Takata, et al., Antiproliferative constituents from Umbelliferae plants VII. Active triterpenes and rosmarinic acid from Centella asiatica, Biol. Pharm. Bull. 28 (2005) 173–175.
[4] K.S. Ahn, M.S. Hahm, E.J. Park, H.K. Lee, I.H. Kim, Corosolic acid isolated from the fruit of Crataegus pinnatifida var. psilosa is a protein kinase C inhibitor as well as a cytotoxic agent, Planta Med. 64 (1998) 468–470.
[5] D.H. Kim, K.M. Han, I.S. Chung, D.K. Kim, S.H. Kim, B.M. Kwon, et al., Triterpenoids from the flower of Campsis grandiflora K. Schum. as human acyl-CoA: cholesterol acyltransferase inhibitors, Arch. Pharm. Res. 28 (2005) 550–556.
[6] N.T. Dat, X.F. Cai, M.C. Rho, H.S. Lee, K. Bae, Y.H. Kim, The inhibition of diacylglycerol acyltransferase by terpenoids from Youngia koidzumiana, Arch. Pharm. Res. 28 (2005) 164–168.
[7] C. Murakami, K. Myoga, R. Kasai, K. Ohtani, T. Kurokawa, S. Ishibashi, et al., Screening of plant constituents for effect on glucose transport activity in Ehrlich ascites tumour cells, Chem. Pharm. Bull. (Tokyo) 41 (1993) 2129–2131.
[8] T. Miura, Y. Itoh, T. Kaneko, N. Ueda, T. Ishida, M. Fukushima, et al., Corosolic acid induces GLUT4 translocation in genetically type 2 diabetic mice, Biol. Pharm. Bull. 27 (2004) 1103–1105.
[9] X. Wen, H. Sun, J. Liu, G. Wu, L. Zhang, X. Wu, et al., Pentacyclic triterpenes. Part 1: the first examples of naturally occurring pentacyclic triterpenes as a new class of inhibitors of glycogen phosphorylases, Bioorg. Med. Chem. Lett. 15 (2005) 4944–4948.
[10] T. Miura, N. Ueda, K. Yamada, M. Fukushima, T. Ishida, T. Kaneko, et al., Antidiabetic effects of corosolic acid in KK-Ay diabetic mice, Biol. Pharm. Bull. 29 (2006) 585–587.
[11] M. Fukushima, F. Matsuyama, N. Ueda, K. Egawa, J. Takemoto, Y. Kajimoto, et al., Effect of corosolic acid on postchallenge plasma glucose levels, Diabetes Res. Clin. Pract. 73 (2006) 174–177.
[12] A. Consoli, Role of liver in pathophysiology of NIDDM, Diabetes Care 15 (1992) 430–441.
[13] E. Ferrannini, L.C. Groop, Hepatic glucose production in insulin-resistant states, Diabetes Metab. Rev. 5 (1989) 711–726.
[14] T. Sugano, K. Suda, M. Shimada, N. Oshino, Biochemical and ultrastructural evaluation of isolated rat liver systems perfused with a hemoglobin-free medium, J. Biochem. (Tokyo) 83 (1978) 995–1007.
[15] Y. Nishimura, Y. Inoue, H. Takeuchi, Y. Oka, Acute effects of pioglitazone on glucose metabolism in perfused rat liver, Acta. Diabetol. 34 (1997) 206–210.
[16] M. Hosokawa, B. Thorens, Glucose release from GLUT2-null hepatocytes: characterization of a major and a minor pathway, Am. J. Physiol. Endocrinol. Metab. 282 (2002) E794–E801.
[17] E. Van Schaftingen, B. Lederer, R. Bartrons, H.G. Hers, Fructose-2,6-bisphosphatase from rat liver, Eur. J. Biochem. 124 (1982) 143–149.
[18] I. Miwa, Y. Mita, T. Murata, J. Okuda, M. Sugiura, Y. Hamada, Utility of 3-O-methyl-N-acetyl-D-glucosamine, an N-acetylglucosamine kinase inhibitor, for accurate assay of glucokinase in pancreatic islets and liver. Enzyme Protein 48 (1994–1995) 135–142.
[19] K. Aoki, T. Saito, S. Satoh, K. Mukasa, M. Kaneshiro, S. Kawasaki, et al., Dehydroepiandrosterone suppresses the elevated hepatic glucose-6-phosphatase and fructose-1,6-bisphosphatase activities in C57BL/Ksj-db/db mice: comparison with troglitazone, Diabetes 48 (1999) 1579–1585.
[20] J.V. Passoneau, O.H. Lowry, Enzymic Analysis: A Practical Guide, Humana Press, Totowa, 1993.
[21] E. Van Schaftingen, L. Hue, H.G. Hers, Fructose 2,6-bisphosphate, the probably structure of the glucose- and glucagon-sensitive stimulator of phosphofructokinase, Biochem. J. 192 (1980) 897–901.
[22] S.J. Pilkis, M.R. El-Maghrabi, J. Pilkis, T.H. Claus, D.A. Cumming, Fructose 2,6-bisphosphate. A new activator of phosphofructokinase, J. Biol. Chem. 256 (1981) 3171–3174.
[23] E. Van Schaftingen, B. Lederer, R. Bartrons, H.G. Hers, A kinetic study of pyrophosphate: fructose-6-phosphate phosphotransferase from potato tubers, Application to a microassay of fructose 2,6-bisphosphate, Eur. J. Biochem. 129 (1982) 191–195.
[24] E. Van Schaftingen, H.G. Hers, Inhibition of fructose-1,6-bisphosphatase by fructose 2,6-biphosphate, Proc. Natl. Acad. Sci. U.S.A. 78 (1981) 2861–2863.
[25] S.J. Pilkis, M.R. el-Maghrabi, T.H. Claus, Hormonal regulation of hepatic gluconeogenesis and glycolysis, Annu. Rev. Biochem. 57 (1988) 755–783.
[26] L. Massa, S. Baltrusch, D.A. Okar, A.J. Lange, S. Lenzen, M. Tiedge, Interaction of 6-phosphofructo-2-kinase/fructose-2, 6-bisphosphatase (PFK-2/FBPase-2) with glucokinase activates glucose phosphorylation and glucose metabolism in insulin-producing cells, Diabetes 53 (2004) 1020–1029.
[27] W.V. Judy, S.P. Hari, W.W. Stogsdill, J.S. Judy, Y.M. Naguib, R. Passwater, Antidiabetic activity of a standardized extract (Glucosol) from Lagerstroemia speciosa leaves in type II diabetics. A dose-dependence study, J. Ethnopharmacol. 87 (2003) 115–117.

Pharmacology, Biochemistry and Behavior 92 (2009) 1–5

Contents lists available at ScienceDirect

Pharmacology, Biochemistry and Behavior

journal homepage: www.elsevier.com/locate/pharmbiochembeh

Levels of *N*-acylethanolamines in O,O,S-trimethylphosphorothioate (OOS-TMP)-treated C57BL/6J mice and potential anti-obesity, anti-diabetic effects of OOS-TMP in hyperphagia and hyperglycemia mouse models

Linfang Huang [a,b], Megumi Toyoshima [b], Akihiro Asakawa [b], Kayoko Inoue [b], Kouji Harada [b], Tomomi Kinoshita [c], Shilin Chen [a], Akio Koizumi [b,*]

[a] Institute of Medicinal Plant Development, Chinese Academy of Medical Sciences & Peking Union Medical College, Beijing 1000193, China
[b] Department of Health and Environmental Sciences, Kyoto University Graduate School of Medicine, Kyoto 606-8501, Japan
[c] Graduate School of Engineering, Kyoto University, Kyoto 606-8510, Japan

ARTICLE INFO

Article history:
Received 3 June 2008
Received in revised form 1 October 2008
Accepted 10 October 2008
Available online 1 November 2008

Keywords:
N-acylethanolamines
O,O,S-trimethylphosphorothioate
Anorexia
GC/MS
db/db mice
Akita mice
Anti-diabetic
Anti-obesity

ABSTRACT

O,O,S-Trimethylphosphorothioate (OOS-TMP) has been shown to induce hypophagia and hypopraxia. Recent studies suggest that OOS-TMP-induced anorexia is partly mediated by its effect on the central nervous system. In this study, we examined the profiles of *N*-acylethanolamines (NEAs), including five amide-linked compounds, in the gastrointestinal system in C57BL/6J (B6) mice. The present results shown an orexigenic profile of the levels of NEAs with downregulation of the anorectic lipid, *N*-stearoylethanolamine (SEA), upregulation of the orexigenic lipid, 2-arachidonoyl glycerol (2-AG), at 2 h and upregulation of 2-AG at 24 h albeit with significant anorexia. However, the data indicated that the high level of 2-AG may be responsible for the hypopraxia. We next explored whether OOS-TMP may affect two models of hyperphagia and hyperglycemia, *ins2*$^{+/Akita}$ B6 (Akita) and B6-*lepr*^{db}/*lepr*^{db} mice (db/db). We identified potential anorexigenic effects in B6, Akita and db/db mice. Moreover, OOS-TMP was found to reduce blood glucose in Akita mice but not in db/db mice. Collectively, these findings suggest that *N*-acylethanolamines are not involved in the hypophagia but rather hypopraxia, and may play multiple physiological roles in this process. OOS-TMP might be a promising candidate for anti-obesity and anti-diabetic drug development.

1. Introduction

O,O,S-trimethylphosphorothioate (OOS-TMP) is a contaminant in a number of widely used organophosphorous insecticides. It has been recognized as a unique environmental and lung toxicant that causes emaciation, lung injury, hypercapnia, hypothermia, hyperethanolaminuria and death owing to wasting without inhibition of AchE activity in mammalian species. (Koizumi et al., 1988; Aldridge et al., 1979; Verschoyle and Cabral, 1982; Imamura et al., 1983a,b; Aldridge et al., 1985; Gandy and Imamura, 1985; Umetsu et al., 1977).

Anorexia is one of the typical symptoms of the wasting syndrome caused by OOS-TMP administered by per os, intracerebroventricular (i.c.v.) or intraperitoneal (i.p.) routes, and is accompanied by hypothermia and hypopraxia (Huang et al., 2007; Ohtaka et al., 1995; Hasegawa and Koizumi, 1990).

Regulation of appetite and body weight is mediated by a complex physiological network involving both the central and peripheral nervous systems (Schwartz et al., 2000). In our previous study, both i.c.v. and i.p. injections transiently induced hypophagia at a dose of 5 mg/kg, with mild bronchial damages without alveolar injury. Hypophagia was accompanied by upregulation of corticotropin releasing factor (CRF) in the hypothalamus. At doses higher than 5 mg/kg, i.c.v. injection induced continuous hypophagia from 20 min to 72 h after dosing, accompanied by hypothermia and lung injury. OOS-TMP is thought to induce hypophagia by enhancing the expression of CRF in the hypothalamus (Huang et al., 2007). However, the role of the peripheral gastrointestinal system in hypophagia remains unclear.

N-acylethanolamines (NAEs) are a group of lipid mediator molecules with a wide range of biological effects. It is generally believed that they are formed from *N*-acylated phosphatidylethanolamines (NAPEs) (Schmid et al., 1990; Hansen et al., 2002; Schmid et al., 2002). Increasing evidence has demonstrated the ability of the *N*-acylethanolamines to control appetite, lipid homeostasis and energy balance. *N*-arachidonoylethanolamine (AEA), 2-arachidonoylglycerol (2-AG), *N*-palmitoylethanolamine (PEA), *N*-oleoylethanolamine (OEA) and *N*-stearoylethanolamine (SEA) belong

Abbreviations: OOS-TMP, O,O,S-trimethylphosphorothioate; i.c.v., intracerebroventricular; NEAs, *N*-acylethanolamines; PEA, *N*-palmitoylethanolamine; OEA, *N*-oleoylethanolamine; AEA, *N*-arachidonoylethanolamine (anandamide); 2-AG, 2-arachidonoyl glycerol; SEA, *N*-stearoylethanolamine; GC/MS, gas chromatography/mass spectrometry.

* Corresponding author. Department of Health and Environmental Sciences, Graduate School of Medicine, Kyoto University, Konoe-cho Yoshida Sakyo-ku Kyoto, 606-8501, Japan. Tel.: +81 75 753 4456; fax: +81 75 753 4458.
E-mail address: koizumi@pbh.med.kyoto-u.ac.jp (A. Koizumi).

0091-3057/$ – see front matter © 2008 Published by Elsevier Inc.
doi:10.1016/j.pbb.2008.10.003

to the family of *N*-acylethanolamines that are generated by the enzyme *N*-acylphosphatidylethanolamine-hydrolyzing phospholipase D. The anandamide (AEA) and 2-AG, the first lipids identified to have orexigenic activities, are the main endogenous agonists of cannabinoid receptors found in the brain and other tissues associated with orexigenic effects (Pagotto and Pasquali, 2005; Engeli et al., 2005; Howlett et al., 2002). In contrast, some other anorectic lipid classes of structurally-related compounds, such as *N*-palmitoylethanolamine (PEA), *N*-oleoylethanolamine (OEA) and *N*-stearoylethanolamine (SEA), have been reported to be involved in the anorectic response (Terrazzino et al., 2004; Schmid et al., 2002).

In light of recent progress in understanding the regulation of eating behavior in the central nervous system, it is interesting to investigate the effects of OOS-TMP on the peripheral *N*-acylethanolamines levels in the gastrointestinal tract. Thus, one of the aims of the present study was to determine the levels of peripheral *N*-acylethanolamines including PEA, OEA, SEA, AEA, 2-AG that are closely associated with appetitive function, lipid homeostasis, behavior and energy balance in mice treated with OOS-TMP. In the present study, we used C57BL/6J (B6) mice, which are genetically more homogenous than ddY mice, which were not derived from an inbred mouse strain.

ins2$^{+/Akita}$ mice, a model of type 2 diabetes (Yoshioka et al., 1997), carries a C96Y mutation in the Ins2 gene on a B6 background (Wang et al., 1999). While B6-*lepr*^{db}/*lepr*^{db} (db/db) mice, a well-established genetic rodent model of hyperphagia, obesity, insulin resistance, is another model of type 2 diabetes (Hummel et al., 1966; Shao et al., 2000). As both of these diabetic models are characterized by hyperglycemia and hyperphagia, we intended to explore whether or not OOS-TMP has an influence in these mice.

2. Methods

2.1. Animals

The study protocol was approved by the Animal Research Committee of Kyoto University. All mice were handled in accordance with the Animal Welfare Guidelines of Kyoto University. We used male mice throughout this study. We purchased B6 and B6 background db/db and diabetic nonobese Akita mice(*ins2*$^{+/Akita}$) from Japan SLC, Inc. (Shizuoka, Japan). A total of 45 mice were housed individually and given free access to a pelletized chow and water during the acclimatization period, except when otherwise indicated. A standard commercial lab chow diet (F-2, 3.73 kcal/g, Funahashi Farm Corp., Chiba, Japan) was used. All animals were maintained at an ambient temperature of 24±2 °C and 50±10% humidity with a 12 h dark–light cycle (lights on at 7:00 AM).

2.2. Chemicals and OOS-TMP

All chemicals were of the purest analytical grade. OOS-TMP was synthesized and purified as previously described by Hasegawa and Koizumi (1990). The purity of the compound was found to be more than 99.8% as determined by NMR (JEOL JNM-EX400KS, JEOL Ltd. Akishima, Tokyo, Japan). PEA, OEA, AEA, 2-AG and SEA were purchased from Cayman Chemical Co. (Ann Arbor, MI).

2.3. i.c.v. cannulation

The surgical operation for i.c.v. cannulation was carried out as reported by Asakawa et al. (2001). Briefly, mice were anesthetized with sodium pentobarbital by i.p. injection (80–85 mg/kg) and fixed in a stereotaxic frame (SR-6, Narishige, Tokyo, Japan). A small hole was made in the skull using a needle inserted 0.9 mm lateral to the central suture and 0.9 mm posterior to the bregma. A 24-gauge cannula beveled at one end over a distance of 3 mm (Safelet-Cas, Nipro, Osaka, Japan) was put into the third cerebral ventricle for i.c.v. injection. The stainless-steel cannula was fixed to the skull with dental cement and capped with silicon without an obtruder. The animals were allowed to recover for 1 week before any experimental manipulation.

To ascertain the injection site that the drugs were injected exactly into the cerebral ventricle, at the end of all i.c.v. experiments, diluted India ink was injected through the cannula and animals were killed immediately by anesthetic overdose. Only those animals showing uniform distribution of ink into the ventricles were used for statistical analysis.

2.4. i.c.v. injection and experimental process

Conscious 7-week old animals were gently restrained by hand. A dose of 5 mg/kg of OOS-TMP was chosen because this dose induced hypophagia by upregulating of CRF without any toxicological signs (Huang et al., 2007). Four microliters of various concentrations of OOS-TMP dissolved in 5% dimethylsulfoxide (DMSO) in 0.9% saline were injected i.c.v. using a microsyringe via PE-20 tubing fitted with a 27-gauge needle that was inserted through the guide cannula to a depth of 3 mm below the external surface of the skull. Control animals received an equivalent volume of vehicle (5% DMSO in 0.9% saline). Before feeding tests, mice were fasted for 16 h with unlimited access to water. OOS-TMP or vehicle was singly administered by i.c.v. to food-deprived mice at 10:00 a.m. Food intake was recorded at 20 min and at 1, 2, 4, 6 and 24 h, and body weights were monitored at 0, 6, 12 and 24 h after i.c.v. injection. To determine the blood glucose levels, blood samples were collected from the tail vein immediately before fasting at between 18:00 and 19:00 pm, and a further sample was obtained from the orbital sinus at 10:00 am, i.e., 24 h after i.c.v. injection. The blood glucose levels were determined using a glucometer (Glutest Ace; Arkray Factory, Shiga, Japan), which used the glucose oxidase method. At the end of observation, mice were sacrificed by rapid decapitation. The intestines were removed quickly, rinsed with 2×1 ml ice-cold saline, and then immediately stored in liquid nitrogen at −70 °C until analyzed. In addition, we obtained and stored the lung to investigate lung injury.

2.5. Gas chromatography/mass spectrometer (GC/MS) analysis of N-acylethanolamines in the intestine

The intestinal content of *N*-acylethanolamines was determined by isotope-dilution GC/MS (Giuffrida and Piomelli, 1998; Felder et al., 1996). Lipid extraction and fractionation were performed as previously described (Schmid et al., 1995; Yang and Karoum, 1999) with a slight modification. Thawed intestine (0.6 g) was homogenized in 20 ml chloroform and spiked with an isotope mixture (5 μl) containing ^{13}C labeled 2-AG, AEA, PEA, SEA and OEA (500 pmol each) as internal standards. Then, 10 ml of 0.5% saline and 10 ml of methanol were added, shaken for 1 h and centrifuged at 15,000 ×g for 15 min. The lipid chloroform fraction was recovered; a further 10 ml of 0.5% saline and 10 ml methanol was added, and the mixture incubated for another 20 min and centrifuged as described above. This step was repeated twice. The lipid chloroform fraction was dried on a rotary evaporator at a temperature below 50 °C. The lipid extract was redissolved in 5 ml of chloroform and applied to a column (Presep-C Florisil, Wako Pure Chemical Industries, Ltd., Osaka, Japan). The lipid extracts were washed with hexane, 0.1% acetic acid in hexane and then 20% ethyl acetate in hexane, and eluted using 2% methanol in chloroform. The fractions eluted in 2% methanol in chloroform were collected and dried with a stream of nitrogen. The dried residues were derivatized by adding100 μL O-Bis(trimethylsilyl)trifluoroacetamide. The vials were tightly capped and heated at 50 °C for 60 min. After cooling to room temperature, the derivatives were dried under nitrogen, reconstituted in 50 μL of chloroform and vortex mixed. The extracts were injected into an Agilent Technologies 6890 N Network GC equipped with an HP-5MS column (30 m×0.25 mm i.d., Hewlett-

Table 1
Effects of a single i.c.v. injection of OOS-TMP (5 mg/kg) on gut lipids (B6)

Time after dosing		Number of mice	Anrexigenic lipids (pmol/g tissue)			Orexigenic lipids (pmol/g tissue)	
			PEA	OEA	SEA	AEA	2AG
2 h	Case	5	63.61±19.59	1.11±1.56	37.85±7.02 *	7.38±0.87	1719.58±599.69
	Controls	5	59.73±11.09	0.74±0.73	52.99±9.00	6.1±0.88	1290.49±119.90
24 h	Case	5	184.93±35.16	85.4622±89.83	13.362±4.97	0.497±0.59	3565.74±1164.00 *
	Control	5	232.83±68.56	200.43±103.35	12.41±5.05	0.93±0.92	1698.21±450.79

$n=5$ per group *$p<0.05$ vs. control.
*Significant ($p<0.05$).

Packard, Palo Alto, CA) in the splitless mode. Mass spectral data were acquired using the Agilent 5973 Network Mass Selective Detector. The oven temperature was increased from 150 °C to 280 °C at a rate of 10 °C per min. The M-15 ions were monitored using the selected ion monitoring mode.

2.6. Statistical analysis

For the levels of *N*-acylethanolamines, statistical analysis was performed using the Wilcoxon signed-rank test. One-way analysis of variance (ANOVA) was used for the cumulative food intake, relative body weight, and blood glucose level. When ANOVA was significant, the Duncan procedure was performed for multiple comparisons. All analyses were done using STATISTICA™ software (StatSoft®, Japan). A p value <0.05 was considered to be significant.

3. Results

3.1. Effects of a single i.c.v. injection of OOS-TMP on the levels of *N*-acylethanolamines in the intestine of B6 mice at 2 h and 24 h

Previous studies have shown that anorexia generated by OOS-TMP is partly mediated by its action on the central nervous system, while the profile of the peripheral gastrointestinal system is currently unclear. Therefore, we determined the levels of *N*-acylethanolamines (NEAs) including PEA, OEA, SEA. AEA, 2-AG fatty acid amide compounds in intestines (peripheral organ) to investigate whether OOS-TMP acts on the gastrointestinal system resulting in anorexia, hypopraxia.

We determined the levels of *N*-acylethanolamines (NEAs) in the intestines at 2 h and 24 h after administration of OOS-TMP. As shown in Table 1, at 2 h, quantification of NEAs by GC/MS revealed that that the level of SEA, an anorexic lipid mediator, was significantly decreased after treatment with OOS-TMP at a dose of 5 mg/kg compared with the control group, while its congeners, the other two types of orexic lipid mediators AEA and 2-AG, were slightly increased. On the other hand, at 24 h, the level of 2-AG, an orexigenic lipid mediator, was further increased (Table 1), while the levels of PEA and OEA, an anorexic molecule, declined to a lesser extent. No detectable changes were observed in SEA compared with the controls (Table 1).

The present results indicated that the orexigenic profile of the endocannabinoid levels was strengthened in the intestine with OOS-TMP at a dose of 5 mg/kg at 2 h and 24 h albeit with significant anorexia.

3.2. Effects of OOS-TMP on cumulative food intake, body weight gain and blood glucose in B6, Akita and db/db mice

Next, we investigated whether OOS-TMP induces comparable anorexigenic effects in the hyperphagic mouse models Akita and db/db mice. OOS-TMP significantly inhibited feeding in B6 at all time points, while feeding in the Akita and db/db mice had recovered somewhat by 4 h, indicating that the effects of OOS-TMP were less intensive in these hyperphagic mice. However, of interest is that at 24 h, OOS-TMP significantly inhibited food intake in these mice (OOS-TMP vs control (g); B6 mice: 0.28±0.4 vs 4.55±1.54; Akita: 1.02±0.45 vs 3.38±0.65; db/db: 1.85±0.21 vs 5.35±0.86; Fig. 1A, B, C). It should be also pointed out that food consumption by Akita mice and db/db mice did not showed hyperphagia when compared with controls. However, the cumulative food consumption at 24 h in treated mice was significantly larger in Akita or db/db than in C57BL/6 ($p<0.05$).

After administration of OOS-TMP, mice displayed weight loss and decreased food intake. In particular, from 12 to 24 h a significant body weight reduction was observed in Akita mice, and db/db mice showed significant body weight loss at 24 h ($p<0.001$). The mean and SD of

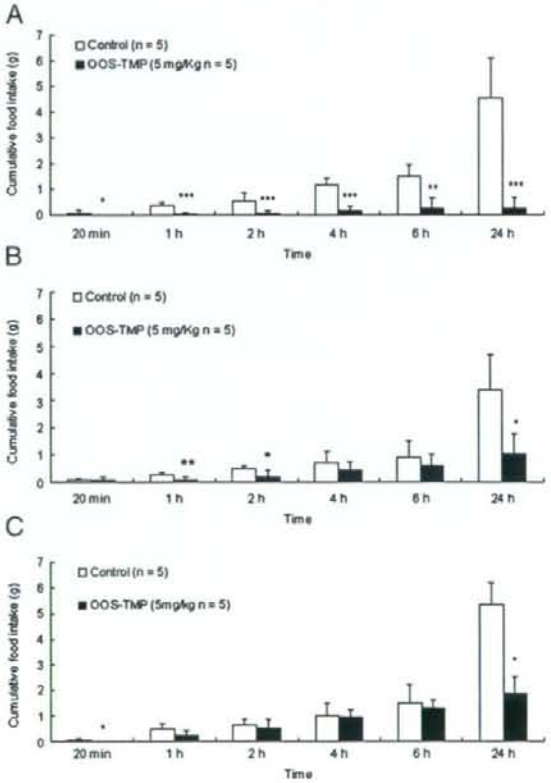

Fig. 1. Effects of a single i.c.v. injection of OOS-TMP (5 mg/kg) on cumulative food intake in B6, Akita and db/db mice from 20 min to 24 h. A. Effect of OOS-TMP on cumulative food intake in food-deprived B6 mice. $n=5$; *$p<0.05$ vs. control, **$p<0.01$ vs. control, ***$p<0.001$ vs. control; B. Effect of OOS-TMP on cumulative food intake in food-deprived Akita mice. $n=5$; *$p<0.05$ vs. control, **$p<0.01$ vs. control, ***$p<0.001$ vs. control; C. Effect of OOS-TMP on cumulative food intake in food-deprived db/db mice $n=5$; *$p<0.05$ vs. control, **$p<0.01$ vs. control, ***$p<0.001$ vs. control.

body weight (g) at 24 h were 23.4±2.25 for B6 mice, 19.98±0.99 for Akita mice and 44.97±1.00 for db/db mice (Fig. 2A,B,C).

Histological examination of the lungs form these mice revealed mild desquamation of the Clara cells in the bronchi as previously reported in ddY mice (Huang et al., 2007) and an absence of alveolar damage at 24 h (data not shown).

Blood glucose levels were significantly decreased at 24 h after OOS-TMP administration in Akita mice ($n=5$); 414.00±96.71 mg/dL before treatment and 138.00±139.40 mg/dL at 24 h after treatment ($p<0.01$). In contrast, blood glucose levels in Akita mice without treatment ($n=5$) were (509.00±90.21 mg/dL) before vehicle treatment and (538.75±70.74 mg/dL) at 24 h after vehicle treatment. In db/db mice, blood glucose levels were ($n=5$); 258.20±74.16 mg/dL before treatment and 347.60±108.34 mg/dL at 24 h after dosing ($p>0.05$) while in db/db control mice, they were (277.75±111.33 mg/dL) and (407.25±157.31 mg/dL) respectively ($p>0.05$).

4. Discussion

Appetite and energy homeostasis are regulated by various stimulatory (orexigenic) and inhibitory (anorexigenic) signaling pathways involving the central nervous system and the gastrointestinal system. Our previous study demonstrated that OOS-TMP induced anorexia, hypopraxia and enhanced the expression of corticotropin releasing factor (CRF), anorexigenic signalling, in the hypothalamus without apparent toxicity (Huang et al., 2007). However, the effects of *N*-acylethanolamines on the intestine have not been investigated. In this paper, sensitive and specific GC/MS assay was used to determine changes in intestinal levels of *N*-acylethanolamines, including PEA, OEA, SEA, AEA and 2-AG.

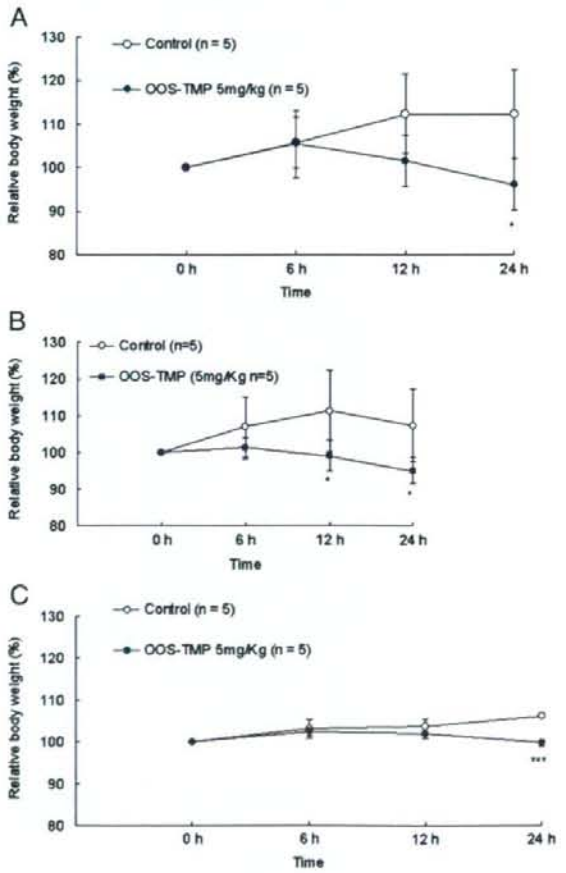

Fig. 2. Effects of a single i.c.v. injection of OOS-TMP (5 mg/kg) on relative body weight of B6 mice, Akita mice and db/db mice from 0 to 24 h. A. Effect of OOS-TMP on relative body weight in food-deprived *B6* mice. $n=5$; $^{*}p<0.05$ *vs.* control, $^{**}p<0.01$ *vs.* control, $^{***}p<0.001$ *vs.* control; B. Effect of OOS-TMP on relative body weight in food-deprived Akita mice. $n=5$ $^{*}p<0.05$ *vs.* control, $^{**}p<0.01$ *vs.* control, $^{***}p<0.001$ *vs.* control; C. Effect of OOS-TMP on relative body weight in food-deprived db/db mice. $n=5$; $^{*}p<0.05$ *vs.* control, $^{**}p<0.01$ *vs.* control, $^{***}p<0.001$ *vs.* control.

It appears that *N*-acylethanolamines signalling via cannabinoid receptors modulates food intake, lipid homeostasis, behaviour and energy balance (Pacher et al., 2006; Cota et al., 2003; Kirkham et al., 2002; Onaivi et al., 2002). Endocannabinoids are implicated in appetite and body weight regulation. 2-AG was the first endocannabinoids to be identified, and is the arachidonate ester of glycerol, which activates both the CB_1 and CB_2 receptors (Mechoulam et al., 1995; Sugiura et al., 1995). Surprisingly, the present study revealed an orexigenic pattern in the intestine at both 2 h and 24 h. Importantly, 2-AG levels remained constantly higher than control at 2 and 24 h conditions, especially, at 24 h, with twofold increase in mice small intestines.

Recently, it has been suggested that 2-AG reduces spontaneous locomotor activity and rearing frequency in a dose-dependent manner (Darmani, 2002). Other studies in rodents have also shown that larger doses of 2-AG and AEA are motor suppressive and both compounds are equipotent in reducing spontaneous locomotor activity (Mechoulam et al., 1995). The present study confirmed that the reduction in locomotor activity requires larger doses of 2-AG as the 2-AG level was1719.58±599.69 pmol/g at 2 h with mice exhibited low locomotor activity and the level at 24 h was 3565.74±1164.00 pmol/g and the mice displayed typical hypopraxia. Given that one of important finding of the present investigation is that the high concentration of 2-AG may be responsible for the reduction in locomotor activity observed, there are two contradictory statuses, in that there was anorexigenic dominance in the central nervous system and orexigenic dominance in the gastrointestinal system. Taken together, it can be concluded that anorexigenic signals in the central nervous system may predominate eating behaviour. By contrast, the endocannabinoid system in the gastrointestinal system may be involved in the locomotor suppression reduced by OOS-TMP.

N-stearoylethanolamine (SEA) has recently been reported also to inhibit food intake by downregulating of liver gene expression of stearoyl-coenzyme A desaturase 1, while PPARα, PPARβ, and PPARγ expression was unaffected (Terrazzino et al., 2004). In the present study, however, we observed an orexigenic profile with significantly declined amount of SEA in intestines at 2 h but unchanged at 24 h after OOS-TMP treatment.

The possible physiological and pathological significance of the changes of *N*-acylethanolamines in the feeding-associated brain region including the hypothalamus, brain stem and limbic forebrain remains to be determined in the future. Particularly, the 2-AG level in the brain needs to be determined because it is found in both the gastrointestinal tract and the brain (Mechoulam et al., 1995).

The present study confirms the previously reported anorexigenic effect of OOS-TMP (Huang et al., 2007; Hasegawa and Koizumi, 1990; Koizumi et al., 1988). However, there are subtle inconsistencies: B6 control mice continued to be hypophagic at 24 h while early recovery in eating behavior was observed in ddY mice (Huang et al., 2007). This discrepancy may indicate a genetic difference in susceptibility to OOS-TMP between these two widely used mice strians. In fact, B6 mice are more genetically homogeneous than ddY mice. Another inconsistency may be related to the absence of hyperphagia in the Akita and db/db control mice that underwent i.c.v. surgery, but without administration of OOS-TMP, when compared with their counterpart control mice. This may be associated with susceptibility to surgery: Akita and db/db might be more susceptible to the damage associated with i.c.v.

surgery. However, when these three types of mice were compared at the 24 h timepoint, the Akita and db/db mice treated with OOS-TMP consumed more diet than the B6 mice ($p<0.05$). Therefore, these results are consistent with our previous observation in that the anorexigenic effects of OOS-TMP in hyperphagic mice, Akita (Toyoshima et al., 2007) and db/db mice were ameliorated compared with wild-type B6 mice.

In our experiment, there was a striking drop in blood glucose in the Akita diabetic mice and a loss of body weight at 24 h, the db/db, Akita and B6 mice after i.c.v. administration of OOS-TMP. This observation suggests that OOS-TMP may have potential anti-obesity and anti-diabetic-like effects in a variety of animal models of eating-related disorders. Comprehensive understanding of the molecular and biochemical mechanism of OOS-TMP-induced anorexia warrants further exploration.

In summary, the present data indicate that peripherally NEAs are not involved in the hypophagia but instead hypopraxia caused by OOS-TMP. We have also shown that the endocannabinoid 2-AG is the most sensitive to variation during feeding. Overall, these findings are consistent with previous reports and support the role of endocannabinoids in the physiological regulation of appetite, body weight and behavior control. Although we observed changes in endocannabinoid levels in the gastrointestinal system after OOS-TMP administration, the exact mechanisms for this remain unknown: it simply represents the fasting conditions in the gastrointestinal system and the effect of OOS-TMP on endocannabinoid metabolizing enzymes left unclear. Further studies are necessary.

Acknowledgements

This work was supported by grants from the Japan International Science and Technology Exchange Center and from the Ministry of Education, Science, Sports and Culture of Japan (for Young Scientists B: 18790378).

References

Aldridge WN, Miles JW, Mount DL, Verschoyle RD. The toxicological properties of impurities in malathion. Arch Toxicol 1979;42:95–100.
Aldridge WN, Dinsdale ED, Nemery B, Verschyole RD. Some aspects of the toxicity of trimethyl and triethyl phosphorothioates. Fundam Appl Toxicol 1985;5:s47–60.
Asakawa A, Inui A, Kaga T, Yuzuriha H, Nagata T, Fujimiya M, et al. A role of ghrelin in neuroendocrine and behavioral responses to stress in mice. Neuroendocrinology 2001;74:143–7.
Cota D, Marsicano G, Tschöp M, Grübler Y, Flachskamm C, Schubert M, et al. The endogenous cannabinoid system affects energy balance via central orexigenic drive and peripheral lipogenesis. J Clin Invest 2003;112:423–31.
Darmani NA. The potent emetogenic effects of the endocannabinoid, 2-AG (2-arachidonoylglycerol) are blocked by Δ9-tetrahydrocannabinol and other cannabinoids. J Pharmacol Exp Ther 2002;1:34–42.
Engeli S, Böhnke J, Feldpausch M, Gorzelniak K, Janke J, Bátkai S, et al. Activation of the peripheral endocannabinoid system in human obesity. Diabetic 2005;54:2838–43.
Felder CC, Nielsen A, Briley EM, Palkovits M, Priller J, Axelrod J, et al. Isolation and measurement of the endogenous cannabinoid receptor agonist, anandamide, in brain and peripheral tissues of human and rat. FEBS Lett 1996;393:231–5.
Gandy J, Imamura T. Cellular responses to O,O,S-trimethyl phosphorothioate-induced pulmonary injury in rats. Toxicol Appl Pharmacol 1985;80:51–7.
Giuffrida A, Piomelli D. Isotope dilution GC/MS determination of anandamide and other fatty acylethanolamides in rat blood plasma. FEBS Lett 1998;422:373–6.
Hansen HS, Moesgaard B, Petersen G, Hansen HH. Putative neuroprotective actions of *N*-acyl-ethanolamines. Pharmacol Ther 2002;95:119–26.
Hasegawa J, Koizumi A. Structure and pulmonary toxicity relationship on O,O-dimethyl *S*-alkyl phosphorothioate esters. Pharmacol Toxicol 1990;66:367–72.
Howlett AC, Barth F, Bonner TI, Cabral G, Casellas P, Devane WA, et al. International Union of Pharmacology classification of cannabinoid receptors. Pharmacol Rev 2002;54:161–202.
Huang LF, Toyoshima M, Asakawa A, Inoue K, Harada K, Kinoshita T, et al. Roles of neuropeptides in O,O,*S*-trimethylphosphorothioate (OOS-TMP)-induced anorexia in mice. Biochem Biophys Res Commun 2007;362:177–82.
Hummel KP, Dickie MM, Coleman DL. Diabetes, a new mutation in the mouse. Science 1966;153:1127–8.
Imamura T, Gandy J, Fukuto TR. Selective inhibition of rat pulmonary monooxygenase by O, O,*S*-trimethyl phosphorothioate treatment. Biochem Pharmacol 1983a;32:3191–5.
Imamura T, Hasegawa L, Gandy J, Fukuto TR. Effect of drug metabolism inducer and inhibitor on O,O,S-trimethyl phosphorothioate induced delayed toxicity in rats. Chem-Biol Interact 1983b;45:53–64.
Kirkham TC, Williams CM, Fezza F, Marzo VD. Endocannabinoid levels in rat limbic forebrain and hypothalamus in relation to fasting,feeding and satiation:stimulation of eating by 2-arachidonoylglycerol. Br J Pharmacol 2002;136:550–7.
Koizumi A, Montalbo M, Nguyen Q, Hasegawa L, Imamura T. Neonatal death and lung injury in rats caused by intrauterine exposure to O,O,S-trimethylphosphorothioate. Arch Toxicol 1988;61:378–86.
Mechoulam R, Ben-Shabat S, Hanus L, Ligumsky M, Kaminski NE, Schatz AR, et al. Identification of an endogenous 2-monoglyceride,present in canine gut, that binds to cannabinoid receptors. Biochem Pharmacol 1995;50:83–90.
Ohtaka K, Hamade N, Yamazaki Y, Suzuki M, Koizumi A. A direct involvement of the central nervous system in hypophagia and inhibition of respiratory rate in rats after treatment with O,O,S-trimethyl phosphorothioate. Arch Toxicol 1995;69:559–64.
Onaivi ES, Leonard CM, Ishiguro H, Zhang PW, Lin ZC, Akinshola BE, Uhl GR. Endocannabinoids and cannabinoid receptor genetics. Prog Neurobiol 2002;66:307–44.
Pacher P, Batkai S, Kunos G. The endocannabinoid system as an emerging target of pharmacotherapy. Pharmacol Rev 2006;58:389–462.
Pagotto U, Pasquali R. Fighting obesity and associated risk factors by antagonising cannabinoid type 1 receptors. The Lancet 2005;365:1363–4.
Schmid HHO, Schmid PC, Natarajan V. *N*-acylated glycerophospholipids and their derivatives. Prog Lipid Res 1990;29:1–43.
Schmid PC, Krebsbach RJ, Perry SR, Dettmer TM, Maasson JL, Schmid HH. Occurrence and postmortem generation of anandamide and other long-chain *N*-acylethanolamines in mammalian brain. FEBS Lett 1995;375(1–2):117–20.
Schmid HHO, Schmid PC, Berdyshev EV. Cell signaling by endocannabinoids and their congeners: questions of selectivity and other challenges. Chem Phys Lipids 2002;121:111–34.
Schwartz MW, Woods SC, Porte DJ, Seeley RJ, Baskin DG. Central nervous system control of food intake. Nature 2000;404:661–71.
Shao J, Yamashita H, Qiao L, Friedman JE. Decreased Akt kinase activity and insulin resistance in C57BL/KsJ-Leprdb/db mice. J Endocrinol 2000;167:107–15.
Sugiura T, Kondo S, Sukagawa A, Nakane S, Shinoda A, Itoh K, et al. 2-Arachidonoylglycerol:apossible endogenous cannabinoid receptor ligand in brain. Biochem Biophys Res Commun 1995;215:89–97.
Terrazzino S, Berto F, Dalle Carbonare M, Fabris M, Guiotto A, Bernardini D, et al. Stearoylethanolamide exerts anorexic effects in mice via down-regulation of liver stearoyl-coenzyme A desaturase-1 mRNA expression. FASEB 2004;18:1580–2.
Toyoshima M, Asakawa A, Fujimiya M, Inoue K, Inoue S, Kinboshi M, et al. Dimorphic gene expression patterns of anorexigenic and orexigenic peptides in hypothalamus account male and female hyperphagia in Akita type 1 diabetic mice. Biochem Biophys Res Commun 2007;19:703–8.
Umetsu N, Grose FH, Allahyari R, Abu-El-Haj S, Fukuto TR. Effect of impurities on the mammalian toxicity of technical malathion and acephate. J Agric Food Chem 1977;25:946–53.
Verschoyle RD, Cabral JRP. Investigation of the acute toxicity of some trimethyl and triethyl phosphorothioates with particular reference to those causing lung damage. Arch Toxicol 1982;51:221–31.
Wang J, Takeuchi T, Tanaka S, Kubo SK, Kayo T, Lu D, et al. A mutation in the insulin 2 gene induces diabetes with severe pancreatic beta-cell dysfunction in the Mody mouse. J Clin Invest 1999;103:27–37.
Yang HYT, Karoum F. GC/MS analysis of anandamide and quantification of *N*-arachidonoylphosphatidyl ethanolamides in various brain regions, spinal cord, testis, and spleen of the rat. J Neurochem 1999;72(5):1959–68.
Yoshioka M, Kayo T, Ikeda T, Koizumi A. A novel locus, Mody4, distal to D7Mit189 on chromosome 7 determines early-onset NIDDM in nonobese C57BL/6 (Akita) mutant mice. Diabetes 1997;46:887–94.

Biochemical and Biophysical Research Communications 371 (2008) 320–323

Contents lists available at ScienceDirect

Biochemical and Biophysical Research Communications

journal homepage: www.elsevier.com/locate/ybbrc

Ablation of *estrogen receptor alpha (ERα)* prevents upregulation of POMC by leptin and insulin

Michi Hirosawa [a], Mutsuko Minata [a], Kouji H. Harada [a], Toshiaki Hitomi [a], Andree Krust [b], Akio Koizumi [a,*]

[a] Department of Health and Environmental Sciences, Kyoto University Graduate School of Medicine, Yoshida Konoe-cho, Sakyo, Kyoto 606-8501, Japan
[b] Institut de Génétique et de Biologie Moléculaire et Cellulaire, Centre National de la Recherche Scientifique, Institut National de la Santé et de la Recherche Médicale, Collège de France, Université Louis Pasteur de Strasbourg, Illkirch, France

ARTICLE INFO

Article history:
Received 15 April 2008
Available online 24 April 2008

Keywords:
Diabetes
Hyperphagia
Dimorphisms
Estrogen receptor alpha

ABSTRACT

Diabetic Akita male mice are more hyperphagic because of downregulation of proopiomelanocortin (POMC) caused by hypoleptinemia. We investigated the role of *estrogen receptor α* (*ERα*) in the regulation of the hypothalamic POMC in females. ERaKOAkt mice consumed 30% greater food (g/3 weeks) than the Akita diabetic controls. Ovariectomized diabetic (AFO) and nondiabetic (B6FO) mice had significantly lower food intake and elevated serum leptin levels. ERaKOAkt and ERaKO mice also increased serum leptin concentrations, while hypoinsulinemia was observed in ERaKOAkt and hyperinsulinemia in ERaKO mice. RT-PCR showed a significant attenuation of *POMC* expression in both ERaKOAkt and ERaKO mice, irrespective of the elevated leptin serum levels or hyperinsulinemia, while elevated serum leptin levels in AFO and B6FO mice upregulated *POMC* gene expression. These results indicate that *ERα* plays an essential role in leptin- and insulin-stimulated upregulation of the *POMC* gene. This action of ERα is likely mediated in a ligand-independent manner.

Diabetes mellitus is one of the most serious health concerns for modern societies and will pose enormous economic burdens on a global level, if effective prevention programs are not initiated. In terms of prevention programs, changing the life-style is essential, as with exercise, diet, and self-monitoring of blood glucose. Of particular importance is controlling the diet. However, a major obstacle to following dietary regimens is hunger [1].

Akita mice (*Ins2*$^{Akita/+}$) carry a C96Y mutation in the *Ins2* gene and spontaneously develop early age-onset diabetes with reduced pancreatic β-cell mass without insulitis or obesity [2–4]. Akita mice are characterized by hyperphagia; males show greater hyperphagia than females [5].

It is well established that the leptin–proopiomelanocortin (POMC) axis plays an important role in appetite control. Leptin is a hormone generated by adipose tissue [6–8], while POMC is one of the major anorexic peptides generated in the hypothalamus [9]. *POMC* expression is upregulated by both insulin [10,11] and leptin [9,12,13]. Our previous study showed that leptin deficiency lowered gene expression of *POMC* in the hypothalamus, leading to hyperphagia in male Akita mice [14]. Hyperphagia and reduced *POMC* gene expression were normalized by castration in males through elevation of leptin [14]. In female Akita mice, the leptin–POMC axis is properly maintained and thus induces only mild hyperphagia [14]. Although sex hormones are speculated to play critical roles in such dimorphic eating behavior, the direct physiological consequence remains largely unknown.

Accumulating evidence indicates that sex hormones act on the regulation of body weight and food intake [15–17]. In particular, the functional roles of estrogen in regulating body fat and metabolic pathways have been extensively studied and recent studies have shown that mice lacking *estrogen receptor alpha* (*ERα*), the main mediator of estrogen effects on energy homeostasis, have increased fat mass and hyperlipidemia [18]. *ERα* expression is involved in the estrogenic control of feeding behavior and weight regulation of female mice [16].

The main aim of the present study was to investigate the effects of estrogen and its receptor ERα on eating behavior. To achieve this, we used *ERα* gene null mice (ERaKOAkt) and ovariectomized (OVX) Akita mice. Here, we report that ERaKOAkt, not ovariectomized Akita mice, showed massive hyperphagia accompanied by reduced gene expression levels of *POMC* in hypothalamus despite elevated serum leptin levels. These results indicate that *ERα* is essential for upregulation of the *POMC* gene by the leptin signaling pathway. This pathway is mediated likely by an estrogen-independent manner.

Materials and methods

Animals. Five-week-old female C57BL/6 and Akita mice were purchased from SLC Japan (Shizuoka, Japan). They were housed under a 12 h:12 h light/darkness cycle in a controlled environment (24 ± 2 °C, 50 ± 10% humidity). *ERα*$^{+/-}$ mice [19]

* Corresponding author. Fax: +81 75 753 4458.
E-mail address: koizumi@pbh.med.kyoto-u.ac.jp (A. Koizumi).

0006-291X/$ - see front matter © 2008 Elsevier Inc. All rights reserved.
doi:10.1016/j.bbrc.2008.04.073

were also housed in the same conditions. To obtain *ERα*-null (ERaKO) and *ERα*-null Akita (ERaKOAkt) mice, male double-heterozygous (*ERα*$^{+/-}$*Akt*) mice were first generated and hybridized with female *ERα*$^{+/-}$ mice. The animals had *ad libitum* access to rodent standard diet (commercial lab chow, F-2; Nippon Clea, Tokyo, Japan) and tap water. All animals were handled in accordance with the Animal Welfare Guidelines of Kyoto University.

Experiments were performed on the following six groups of mice: (1) ERaKO, (2) ERaKOAkt, (3) sham-operated Akita (AFC), (4) OVX Akita (AFO), (5) sham-operated controls (B6F), and (6) OVX controls (B6FO). Each group was composed of six animals except AFC, in which five animals were used. OVX mice were bilaterally OVX under anesthesia (2% avertin, 0.2 ml/ 10 g body weight, ip) (Sigma, Japan). The sham-operated animals were subjected to the same general surgical procedure except ovariectomy. Body weight (BW) and blood glucose (BG) were monitored weekly from 6 weeks of age until the end of the study. All mice were housed individually and food intake (FI) was monitored twice a week at 10 o'clock in the morning.

At 12 weeks of age, mice were killed by decapitation following overnight fasting for 16 h. Hypothalamus and adipose tissues were collected. Blood samples were obtained from the orbital sinus and serum was separated by centrifugation. Serum and tissues samples were stored at −80 °C until analysis.

Measurement of insulin and leptin. Mouse serum insulin and leptin concentrations were measured by ELISA at Nagahama Life Science Laboratory, Oriental Yeast Co. Ltd. (Shiga, Japan).

Quantitative RT-PCR analysis in the hypothalamus. Total RNA was extracted from hypothalamus using RNeasy Lipid Tissue Mini Kit (Qiagen, Japan). Aliquots (10 ng) were amplified using QuantiTect® SYBR® Green RT-PCR (Qiagen, Japan). Quantification of the amplified products was performed on an the 7300 Real-Time PCR system purchased from Applied Biosystems Japan, Ltd. (Tokyo, Japan). All expression data were normalized to mouse glyceraldehyde 3-phosphate dehydrogenase (*G3PDH*) expression level from the same individual sample. The following primers were used for RT-PCR: GAPDH forward, ATGGTGAAGGTCGGTGTGAA and reverse, GAGT GGAGTCATACTGGAAC; POMC forward, GGCTTGCAAACTCGACCTCT and reverse, TGACCCATGACGTACTTCCG.

Data analysis. Data are presented as means ± SD, except for hypothalamic peptides. Since the relative abundance of hypothalamic POMC obtained by RT-PCR was distributed skewly, statistical analyses were conducted after logarithmic transformation. These values are presented as geometric means (GMs) and geometric standard deviations (GSDs). Statistical analyses were done by *t*-test using STATISTICA™ software (StatSoft®, Japan). A *p*-value <0.05 was considered to be significant.

Results

Hyperphagia in ERα-null mice

Daily food consumption in ERaKOAkt and ERaKO mice was monitored from 6 to 12 weeks of age, and compared with their controls, AFC and B6F mice, respectively (Fig. 1A). The ERaKOAkt group was hyperphagic relative to AFC for the duration of the experiment. The levels of hyperphagia in ERaKOAkt female mice were comparable to those in male Akita mice (Data not shown) [14]. The average cumulative food consumption in the ERaKOAkt and ERaKO groups for both 6–9 and 9–12 weeks was significantly increased compared with their corresponding controls (Fig. 1B). These results indicate that ablation of *ERα* induces both mild hyperphagia in nondiabetic mice and massive hyperphagia in insulin deficient mice.

Ovariectomy decreased food intake in diabetic and nondiabetic mice

To determine the role of estrogen, a ligand for ERα, in food consumption, Akita (AFO) and C57BL/6 mice (B6FO) were ovariectomized at 6 weeks of age, and food consumption was measured. In all the groups, changes in food consumption (g/week) at 12 weeks of age, the time at which OVX mice recovered from the operation, were compared with those at 8 weeks. Ovariectomy decreased food consumption in AFO and B6FO mice compared with the corresponding controls (Fig. 2).

Serum insulin and leptin levels

To examine the effects of ERα or estrogen on serum insulin and leptin levels, we measured the serum insulin and leptin levels at 12 weeks of age (Fig. 3). In the mice with Akita background (Fig. 3A, left), ERaKOAkt, AFC, and AFO mice showed a similar degree hypoinsulinemia relative to their hyperglycemia at 12 weeks of age: 589 ± 4.61 (mg/dl) for ERaKOAkt, 420 ± 39.20 for AFC, and 458 ± 40.95 for AFO. On the other hand, in nondiabetic mice (Fig. 3A, right), the ERaKO group showed an increased insulin concentration compared with the B6F group. Their blood glucose levels at 12 weeks of age were: 124 ± 13.01 for ERaKO, 97.5 ± 16.78 for B6F, and 102.9 ± 11.60 for B6FO.

With regard to leptin levels, the ERaKOAkt and AFO mice had significantly higher leptin levels compared with AFC mice (Fig. 3B, left). There was also a similar but greater elevation of leptin levels in nondiabetic animals (Fig. 3B, right). Consistent with this finding, the white adipose weight was increased in ERaKO and B6FO mice (data not shown). Both the ablation of *ERα* or deletion of estrogen by OVX led to increased leptin levels in Akita and nondiabetic mice.

Hypothalamic POMC gene expression

We assessed the levels of hypothalamic neuropeptides, which regulate appetite via leptin signaling. POMC, a major anorexigenic neuropeptide, was measured by quantitative real-time RT-PCR

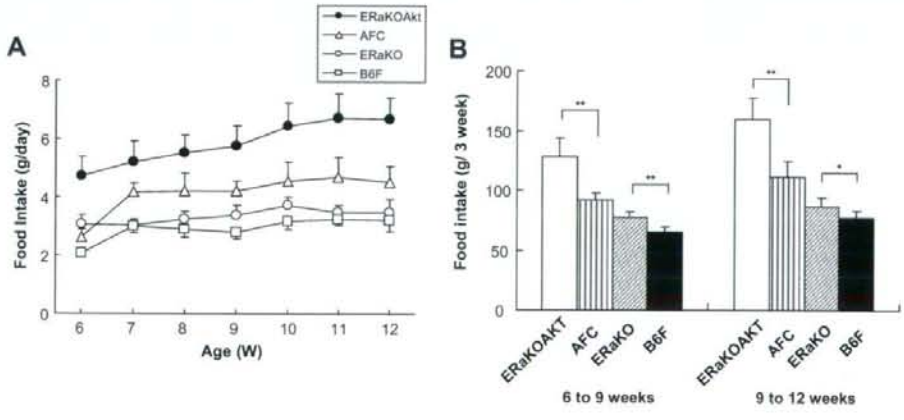

Fig. 1. Effects of *ERα* knockout on food intake in Akita and C57BL/6 mice. Food intake (g/day) (A) and cumulative food intake (g/3 weeks) (B) of Akita females (AFC; $n = 5$), *ERα*$^{-/-}$ Akita females (ERaKOAkt; $n = 6$), C57BL/6 females (B6F; $n = 6$), and *ERα*-null females (ERaKO; $n = 6$) were measured from 6 to 12 weeks of age. All values are expressed as means ± SD. Comparisons were made between ERaKOAkt and AFC, and ERaKO and B6F mice. A $p < 0.05$ was considered to be significant; $^{*}p < 0.05$, $^{**}p < 0.01$.

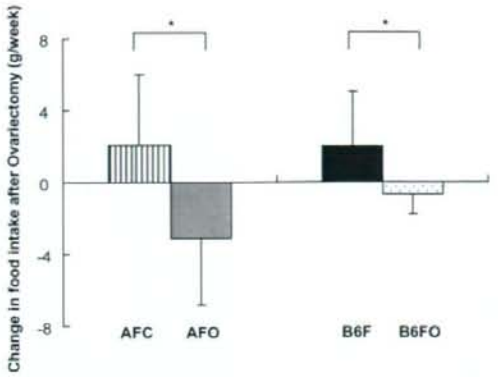

Fig. 2. Effect of ovariectomy on weekly food intake in Akita and C57BL/6 mice. Changes in weekly food intake at 11–12 weeks of age in ovariectomized Akita females (AFO; $n = 6$) and C57BL/6 females (B6FO; $n = 6$), and their respective controls (AFC; $n = 5$ and B6F; $n = 6$) were measured based on their own food intake at 7–8 weeks of age. Values were compared between AFO and AFC, and B6FO and B6F mice. Data are expressed as means ± SD. A $p < 0.05$ was considered to be significant. * $p < 0.05$.

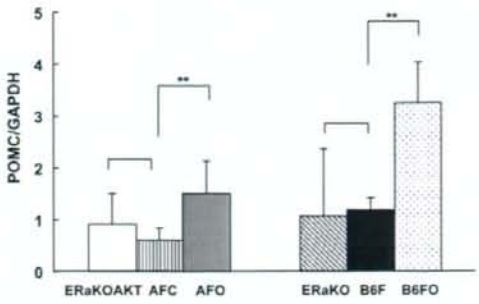

Fig. 4. Relative expression of POMC neuropeptides in hypothalamus. Results are represented as GM and (GMs × GSDs). Expression of POMC was standardized by that of GAPDH. Values were compared as they were in Fig 3. A $p < 0.05$ was considered to be significant. ** $p < 0.01$.

(Fig. 4). In accordance with the elevated serum leptin levels, *POMC* mRNA expression was significantly upregulated in ovariectomized mice, i.e., AFO and B6FO, relative to the corresponding controls (i.e., AFC and B6F, respectively) (Fig. 4). In contrast, ablation of *ERα* markedly attenuated leptin-mediated upregulation of *POMC* transcription, as shown in ERaKOAkt or ERaKO mice compared with AFO or B6FO mice, respectively although all had elevated serum leptin levels (Fig. 4).

These findings indicate that *ERα* is essential for transferring leptin signals to the *POMC* gene. The attenuated response of the *POMC* gene in the hypothalamus seems to be associated with hyperphagia in ERaKOAkt and ERaKO mice, although the degree of hyperphagia is more prominent in the former than in the latter, suggesting that insulin can suppress appetite in the latter via pathways other than insulin–POMC axis.

Discussion

In the present study, we confirmed that ablation of the estrogen signaling pathway either by ovariectomy or deletion of *ERα* increased serum leptin levels, as previously reported [16,17]. Interestingly, however, the increased serum leptin levels did not upregulate *POMC* gene expression in the hypothalamus in *ERα*-null mice; *ERα* ablation was found to attenuate the upregulation of the *POMC* gene in response to increased leptin signals, while ablation of estrogen by OVX maintained the response. Attenuation of the *POMC* response to leptin signals was found in both diabetic and nondiabetic *ERα*-null mice, irrespective of insulin levels.

Insulin stimulates *POMC* mRNA expression via the phosphatidylinositol 3-kinase (PI3K) to forkhead-O-transcription factor (FoxO1) signaling pathway, while leptin stimulates POMC expression via the Janus kinases and signal transducer and activators of transcription (JAK-STAT) pathway [11]. Regulation of *POMC* gene expression by FoxO1 and STAT3 is mediated by binding to adjacent sites in its two promoters [20]. If so, the insulin and leptin signaling pathways are independent. The present data strongly indicate that ERα plays a critical role in signal transduction in both pathways, based on the observation that destruction of *ERα* attenuated *POMC* gene expression in ERaKOAkt which has elevated serum leptin levels and hypoinsulinemia, and ERaKO mice, which has elevated serum leptin levels and hyperinsulinemia. We believe that this is the first definitive *in vivo* evidence showing the regulatory role of ERα in upregulation of *POMC* gene expression mediated by leptin or insulin.

ERα is a member of a superfamily of nuclear steroid hormone receptors, which can regulate the transcriptional activity of target genes by interacting with different DNA response elements. In addition to mediating the classic transcriptional effects of estrogen, ERα can be transcriptionally activated in the absence of estrogen, a process referred to as ligand-independent activation [21]. Recently,

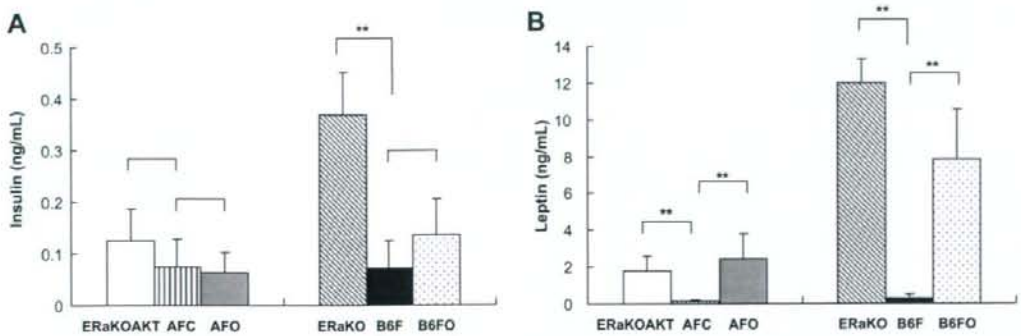

Fig. 3. Serum levels of insulin (A) and leptin (B) in diabetic mice (ERaKOAkt, AFC, and AFO) 15 and nondiabetic mice (ERaKO, B6F, and B6FO). Blood was collected after overnight fast for 16 h. Values were compared between AFC and ERaKOAkt or AFO and between B6F and ERaKO or B6FO mice. Data are expressed as means ± SD. A $p < 0.05$ was considered to be significant. ** $p < 0.01$.

Catalano et al. showed that leptin activates the ERα *per se* through the mitogen-activated protein kinase (MAPK) pathway in a ligand-independent manner *in vitro* [21]. They demonstrated that unliganded ERα is an effector of the MAPK signal and leptin can, via Janus kinase 2, activate the Ras-dependent MAPK pathway. Along this line, our study implies that unliganded ERα mediates POMC upregulation by leptin. To the best of our knowledge, this is the first *in vivo* evidence for the role of unliganded ERα in the regulation of *POMC* gene expression, although further studies are needed to elucidate the involvement of *ERα*.

The extent of hyperphagia, however, was much less predominant in ERaKO than in ERaKOAkt mice, which is comparable with male Akita diabetic mice, with the latter showing hypoinsulinemia and the former showing hyperinsulinemia. Differences in food consumption between the two ERaKO groups may be explained by the contribution of insulin. Insulin-dependent downregulation of orexigenic signals, such as AgRP, [11], may prevent massive hyperphagia in ERaKO mice, while they are ineffective in hypoinsulinemic conditions such as ERaKOAkt mice. If this is the case, this insulin dependent downregulation is not mediated by ERα. Although the details of the underlying mechanisms remain unknown, the current difference in consumption of food between ERaKO and ERaKOAkt mice warrants further analysis in future studies.

In conclusion, our data demonstrated a novel estrogen-independent action of ERα in the regulation of *POMC* gene expression. This observation may provide important information about the mechanisms modulating eating behavior, which will broaden the clinical approach in diabetic patients in future.

Acknowledgments

This study was supported by a Grant from the Ministry of Education, Science, Sports and Culture of Japan (Kiban Kenkyuu S: 17109007 and Wakate Kenkyuu B: 18790378).

References

[1] D.G. Schlundt, M.R. Rea, S.S. Kline, J.W. Pichert, Situational obstacles to dietary adherence for adults with diabetes, J. Am. Diet. Assoc. 94 (1994) 874–876, 879; quiz 877–878.
[2] M. Yoshioka, T. Kayo, T. Ikeda, A. Koizumi, A novel locus, Mody4, distal to D7Mit189 on chromosome 7 determines early-onset NIDDM in nonobese C57BL/6 (Akita) mutant mice, Diabetes 46 (1997) 887–894.
[3] J. Wang, T. Takeuchi, S. Tanaka, S.K. Kubo, T. Kayo, D. Lu, K. Takata, A. Koizumi, T. Izumi, A mutation in the insulin 2 gene induces diabetes with severe pancreatic beta-cell dysfunction in the Mody mouse, J. Clin. Invest. 103 (1999) 27–37.
[4] T. Kayo, A. Koizumi, Mapping of murine diabetogenic gene mody on chromosome 7 at D7Mit258 and its involvement in pancreatic islet and beta cell development during the perinatal period, J. Clin. Invest. 101 (1998) 2112–2118.
[5] A. Asakawa, M. Toyoshima, K. Inoue, A. Koizumi, Ins2Akita mice exhibit hyperphagia and anxiety behavior via the melanocortin system, Int. J. Mol. Med. 19 (2007) 649–652.
[6] J.M. Friedman, J.L. Halaas, Leptin and the regulation of body weight in mammals, Nature 395 (1998) 763–770.
[7] F. Lonnqvist, P. Arner, L. Nordfors, M. Schalling, Overexpression of the obese (ob) gene in adipose tissue of human obese subjects, Nat. Med. 1 (1995) 950–953.
[8] M. Maffei, J. Halaas, E. Ravussin, R.E. Pratley, G.H. Lee, Y. Zhang, H. Fei, S. Kim, R. Lallone, S. Ranganathan, et al., Leptin levels in human and rodent: measurement of plasma leptin and ob RNA in obese and weight-reduced subjects, Nat. Med. 1 (1995) 1155–1161.
[9] S.F. Leibowitz, K.E. Wortley, Hypothalamic control of energy balance: different peptides, different functions, Peptides 25 (2004) 473–504.
[10] P.J. Havel, T.M. Hahn, D.K. Sindelar, D.G. Baskin, M.F. Dallman, D.S. Weigle, M.W. Schwartz, Effects of streptozotocin-induced diabetes and insulin treatment on the hypothalamic melanocortin system and muscle uncoupling protein 3 expression in rats, Diabetes 49 (2000) 244–252.
[11] L. Plum, B.F. Belgardt, J.C. Bruning, Central insulin action in energy and glucose homeostasis, J. Clin. Invest. 116 (2006) 1761–1766.
[12] M.A. Cowley, J.L. Smart, M. Rubinstein, M.G. Cerdan, S. Diano, T.L. Horvath, R.D. Cone, M.J. Low, Leptin activates anorexigenic POMC neurons through a neural network in the arcuate nucleus, Nature 411 (2001) 480–484.
[13] J.E. Thornton, C.C. Cheung, D.K. Clifton, R.A. Steiner, Regulation of hypothalamic proopiomelanocortin mRNA by leptin in ob/ob mice, Endocrinology 138 (1997) 5063–5066.
[14] M. Toyoshima, A. Asakawa, M. Fujimiya, K. Inoue, S. Inoue, M. Kinboshi, A. Koizumi, Dimorphic gene expression patterns of anorexigenic and orexigenic peptides in hypothalamus account male and female hyperphagia in Akita type 1 diabetic mice, Biochem. Biophys. Res. Commun. 352 (2007) 703–708.
[15] S. Jeong, M. Han, H. Lee, M. Kim, J. Kim, C.J. Nicol, B.H. Kim, J.H. Choi, K.H. Nam, G.T. Oh, M. Yoon, Effects of fenofibrate on high-fat diet-induced body weight gain and adiposity in female C57BL/6J mice, Metabolism 53 (2004) 1284–1289.
[16] N. Geary, L. Asarian, K.S. Korach, D.W. Pfaff, S. Ogawa, Deficits in E2-dependent control of feeding, weight gain, and cholecystokinin satiation in ER-alpha null mice, Endocrinology 142 (2001) 4751–4757.
[17] R. Meli, M. Pacilio, G.M. Raso, E. Esposito, A. Coppola, A. Nasti, C. Di Carlo, C. Nappi, R. Di Carlo, Estrogen and raloxifene modulate leptin and its receptor in hypothalamus and adipose tissue from ovariectomized rats, Endocrinology 145 (2004) 3115–3121.
[18] P.A. Heine, J.A. Taylor, G.A. Iwamoto, D.B. Lubahn, P.S. Cooke, Increased adipose tissue in male and female estrogen receptor-alpha knockout mice, Proc. Natl. Acad. Sci. USA 97 (2000) 12729–12734.
[19] S. Dupont, A. Krust, A. Gansmuller, A. Dierich, P. Chambon, M. Mark, Effect of single and compound knockouts of estrogen receptors alpha (ERalpha) and beta (ERbeta) on mouse reproductive phenotypes, Development 127 (2000) 4277–4291.
[20] T. Kitamura, Y. Feng, Y.I. Kitamura, S.C. Chua Jr., A.W. Xu, G.S. Barsh, L. Rossetti, D. Accili, Forkhead protein FoxO1 mediates Agrp-dependent effects of leptin on food intake, Nat. Med. 12 (2006) 534–540.
[21] S. Catalano, L. Mauro, S. Marsico, C. Giordano, P. Rizza, V. Rago, D. Montanaro, M. Maggiolini, M.L. Panno, S. Ando, Leptin induces, via ERK1/ERK2 signal, functional activation of estrogen receptor alpha in MCF-7 cells, J. Biol. Chem. 279 (2004) 19908–19915.

Absence of Association between *COL1A1* Polymorphisms and High Myopia in the Japanese Population

Hideo Nakanishi,[1,2] *Ryo Yamada,*[2,3] *Norimoto Gotoh,*[1,2] *Hisako Hayashi,*[1,2] *Atsushi Otani,*[1] *Akitaka Tsujikawa,*[1] *Kenji Yamashiro,*[1] *Noriaki Shimada,*[4] *Kyoko Ohno-Matsui,*[4] *Manabu Mochizuki,*[4] *Masaaki Saito,*[5] *Kuniharu Saito,*[5] *Tomohiro Iida,*[5] *Fumihiko Matsuda,*[2,6] *and Nagahisa Yoshimura*[1]

Purpose. The collagen type I alpha 1 (*COL1A1*) gene was recently reported to be associated with high myopia in the Japanese population. To validate this positive association, the tag single-nucleotide polymorphism (tSNP) approach was used.

Methods. Eight tSNPs, including rs2075555 and rs2269336 (previously reported to be high myopia–susceptible SNPs in the Japanese), were selected to tag the linkage disequilibrium blocks harboring the *COL1A1*. These tSNPs were genotyped by using an SNP assay. A total of 427 unrelated Japanese cases with high myopia (axial length, ≥26.50 mm in both eyes; the refraction of the 644 phakic eyes ranged from −5.0 to −36.0 D, with a mean ± SD of −13.61 ± 4.20 D) and 420 Japanese control subjects were recruited. Genotype and allele distributions were compared between the cases and controls by using the χ^2 test, with multiple testing corrections performed by the permutation test.

Results. There was no association noted between high myopia and rs2075555 ($P = 0.47$, $P_c > 0.99$) and rs2269336 ($P = 0.40$, $P_c > 0.99$). Meta-analysis of a previous Japanese study and new data obtained in a fixed-effect model indicated a mild significant association of high myopia with rs2075555 (odds ratio [OR], 1.19; 95% confidence interval [CI], 1.03–1.38, $P = 0.022$) and rs2269336 (OR, 1.18; 95% CI, 1.02–1.36, $P = 0.026$). No significant associations were seen with further tSNPs tests.

Conclusions. This study did not replicate the previously reported positive association between *COL1A1* and high myopia in the Japanese population, and thus the genetic risk associated with this gene, if any, is weaker than originally reported. (*Invest Ophthalmol Vis Sci.* 2009;50:544–550) DOI:10.1167/iovs.08-2425

Myopia is a common ocular disorder that is found worldwide. The most important contributor to myopic refraction is the axial length of the eyeball (i.e., longer eyes are more myopic),[1–3] and when the elongation of the eyeball is excessive, the condition is called high myopia. It is well known that high myopia is associated with many ocular complications[4] and is one of the major causes of blindness in many developed countries.[5–10] Thus, the economic and social burden of high myopia is an important public health problem.

Recent population-based studies have estimated the prevalence of high myopia in the elderly population to be approximately 1% to 5%,[2,11–16] and this prevalence has been increasing worldwide, especially in the younger East Asian population.[17–19] One possible explanation for the increase in high myopia in developed countries is a change in lifestyle. It has been reported that environmental factors such as near work and higher education can contribute to the development of high myopia. However, genetic factors also have been reported to be responsible for the development of high myopia[20] (for detailed review, see Refs. 21, 22). For example, several twin studies have shown that there is a high heritability of refraction and axial length.[23–28] There have been many studies in which investigators have attempted to use a genetic approach to identify the susceptible locus or genes for high myopia (for detailed review, see Refs. 22, 29, 30), with several genes now reported to have an association.[31–39] However, there are other studies in which the original findings for these genes were not replicated.[25,38,40–48]

Many animal studies on myopia have indicated that there is a local control mechanism of eye growth; hyperopic defocus produces signals from the retina through the retinal pigment epithelium and choroid to cause remodeling of the scleral tissue, and the secondary scleral remodeling results in axial elongation (for detailed review, see Refs. 21, 22, 49, 50). In mammals, the scleral tissue contains approximately 90% collagen by weight, predominantly type I[51] (Zorn M, et al. *IOVS* 1992;33:ARVO Abstract 1811; Norton TT, et al. *IOVS* 1995;36: ARVO Abstract 3517). Several animal studies have reported that mRNA expression of type I collagen in the sclera is reduced during the development of myopia.[52,53] The *COL1A1* (collagen type I, alpha 1) gene encodes the pro-α1 chains of type I collagen. This *COL1A1* is located on 17q21.33, where a myopia susceptibility locus (MYP5, 17q21-22) has been reported.[54] These pathologic, expression, and genetic studies indicated that *COL1A1* is a good candidate gene for myopia. In 2007, Inamori et al.[36] reported that the single-nucleotide polymorphisms (SNPs) rs2075555 and rs2269336 in *COL1A1* are significantly associated with high myopia in the Japanese population. However, Liang et al.[44] reported that the polymor-

From the [1]Department of Ophthalmology and Visual Sciences, and the [2]Center for Genomic Medicine, Kyoto University Graduate School of Medicine, Kyoto, Japan; the [3]Human Genome Center, Institute of Medical Science, University of Tokyo, Tokyo, Japan; the [4]Department of Ophthalmology and Visual Science, Tokyo Medical and Dental University Graduate School, Tokyo, Japan; the [5]Department of Ophthalmology, Fukushima Medical University, Fukushima, Japan; and the [6]Centre National de Génotypage, Evry, France.

Supported in part by the Ministry of Education, Culture, Sports, Science and Technology of Japan and by the Japanese National Society for the Prevention of Blindness.

Submitted for publication June 12, 2008; revised July 28 and August 26, 2008; accepted December 3, 2008.

Disclosure: **H. Nakanishi**, None; **R. Yamada**, None; **N. Gotoh**, None; **H. Hayashi**, None; **A. Otani**, None; **A. Tsujikawa**, None; **K. Yamashiro**, None; **N. Shimada**, None; **K. Ohno-Matsui**, None; **M. Mochizuki**, None; **M. Saito**, None; **K. Saito**, None; **T. Iida**, None; **F. Matsuda**, None; **N. Yoshimura**, None

The publication costs of this article were defrayed in part by page charge payment. This article must therefore be marked "*advertisement*" in accordance with 18 U.S.C. §1734 solely to indicate this fact.

Corresponding author: Nagahisa Yoshimura, Department of Ophthalmology and Visual Sciences, Kyoto University Graduate School of Medicine Shogoinkawaharacho 54, Sakyo, Kyoto, Japan; nagaeye@kuhp.kyoto-u.ac.jp.

phisms of *COL1A1* are not significantly associated with high myopia in the Taiwanese population.

In the present study, we conducted a systematic case-control study to validate the association between the polymorphisms of the *COL1A1* gene (including previously reported susceptible SNPs) and high myopia in the Japanese population.

Methods

All investigations in this study adhered to the tenets of the Declaration of Helsinki. The Institutional Review Board and the Ethics Committee of the each institute approved the protocols of this study. All the patients were fully informed of the purpose and procedures of this study, and written consent was received from each patient.

Study Population

A total of 427 unrelated Japanese patients with high myopia (mean age ± SD, 57.6 ± 14.1 years; men/women, 31.4% vs. 68.6%) were recruited from the Center for Macular Diseases of Kyoto University Hospital, Fukushima Medical University Hospital, and the high myopia clinic of Tokyo Medical and Dental University Hospital. All underwent comprehensive ophthalmic examinations, including dilated indirect and contact lens slit lamp biomicroscopy, automatic objective refraction evaluation, and measurement of the axial length by applanation A-scan ultrasound (UD-6000; Tomey, Nagoya, Japan) or partial coherence interferometry (IOLMaster; Carl Zeiss Meditec, Dublin, CA). To be enrolled in the study, the patients with high myopia were required to have an axial length of ≥26.50 mm in both eyes. The axial lengths of the 854 eyes ranged from 26.50 to 36.32 mm (mean ± SD, 29.18 ± 1.68). Among the 854 eyes enrolled, 644 (75.4%) were phakic, 185 (21.7%) were pseudophakic, and 25 (2.9%) were aphakic. The mean refraction of the 644 phakic eyes ranged from −5.00 to −36.00 D (mean ± SD, −13.61 ± 4.20). To check the results in another axial length-based definition of high myopia, a subset with longer axial lengths was also defined. The inclusion criterion for this subset was axial length ≥ 28.00 mm in both eyes. A total of 278 patients were enrolled in this subset. The axial length of the 556 eyes in this subset was 29.95 ± 1.43 mm. There were 394 phakic eyes in this subset, with the refraction ranging from −7.25 to −36.00 D (−15.03 ± 4.14). If subjects had preexisting ocular diseases or a history of ocular surgery, with the exception of cataract surgery, they were excluded from the study.

As a population-based control, DNA samples from 420 subjects (mean age ± SD, 44.3 ± 12.1 years; men/women, 46.2% vs. 53.8%) were randomly selected from the Pharma SNP Consortium. The cohort had been recruited for previous genomic studies and was regarded as being representative of the general Japanese population.[55] All participants were Japanese and none of the subjects had any history of ocular diseases.

SNP Selection and Genotyping

To replicate the positive association of the SNPs with high myopia that has been reported in a previous Japanese study, we genotyped rs2075555 from intron 11 of the *COL1A1*, and rs2269336 from the 5′ upstream region of the *COL1A1*. The associated functions for these two SNPs have yet to be elucidated. To systematically examine the possible association between the polymorphisms of the *COL1A1* gene and the high myopic cases, we used the tag SNP (tSNP) approach. The public dbSNP database build 126 and the HapMap database phase 2 release 22 were used to extract the relevant sequencing information for the *COL1A1* gene and the genotyping information for the SNPs. Haplotypes and linkage disequilibrium (LD) blocks were inferred by a solid spine of LD with a minimum D′ of 0.8, according to Haploview version 4.0.[56] We selected eight tSNPs to tag the LD blocks harbored within and surrounding the *COL1A1* gene (Fig. 1A). Tagging of the LD blocks was based on the software Tagger (http://www.broad.mit.edu/mpg/tagger/ provided in the public domain by the Broad Institute, Massachusetts of Technology, Cambridge, MA), which used a minimum r^2 of 0.8 and a minimum minor allele frequency (MAF) of 20% in the Japanese population of the HapMap dataset. It has been reported in a Japanese study that two SNPs (rs2075555 and rs2269336) are high myopia–susceptible polymorphisms.[56] These SNPs were both included within the eight tSNPs. Genomic DNA was extracted from the leukocytes of the peripheral blood and purified (QuickGene-810; Fujifilm, Tokyo, Japan). All the tSNPs were genotyped with an SNP assay (*Taq*man; Applied Biosystems, Foster City, CA), according to the manufacturer's instruction.

Statistics

The statistical power calculation was performed using the module case-control for discrete traits of the Genetic Power Calculator (http://pngu.mgh.harvard.edu/~purcell/gpc/ provided in the public domain by the Psychiatric and Neurodevelopmental Genetics Unit, Massachusetts General Hospital, Harvard Medical School, Boston, MA).[57] For the calculation, the type 1 error rate was set at 0.05 and the prevalence of high myopia in the general population was set at 1%. The HWE for the genotype distributions was examined by using the χ^2 test in each group. Differences in the observed genotype and allelic frequencies between the cases with high myopia and the control subjects were also examined by the χ^2 test. For the current experiment, we combined our results for the single SNP analysis of rs2075555 and rs2269336 with the results of a previous Japanese study,[56] in which the Mantel-Haenszel method based on the fixed-effect model was used to elucidate their predisposing effects on high myopia in a larger Japanese population. We performed the meta-analysis using the R software package Meta (http://cran.r-project.org/web/packages/rmeta/index.html/ provided in the public domain by The Comprehensive R Archive Network, hosted by the Department of Statistics and Mathematics, University of Vienna, Austria).

Differences in the estimated haplotype frequencies between the cases and the controls were also examined by the χ^2 test. These SNP and haplotype analyses were performed with Haploview ver. 4.0. The multiple testing correction for P (P_c) was performed by the permutation test (number of iterations, 10,000), also in Haploview, ver. 4.0. The level of statistical significance was set at $P < 0.05$ and $P_c < 0.05$.

Results

The distribution of the genotypes for the eight tSNPs among the cases with high myopia and the control subjects were all in HWE ($P > 0.05$). The results of the genotyping for rs2075555 and rs2269336 in the cases with high myopia and the control subjects are shown in Table 1. In this study, there were no significant differences noted for the genotype and allelic frequencies for these two SNPs in the *COL1A1* gene between the patient and the control cases. The results of the meta-analysis for rs2075555 and rs2269336 are shown in Table 2. The Mantel-Haenszel method showed the summary odds ratio (OR) to be 1.19 (95% confidence interval [CI], 1.03–1.38; $P = 0.022$) for rs2075555 and 1.18 (95% CI, 1.02–1.36; $P = 0.026$) for rs2269336, respectively. When we performed the subset analysis on the 278 cases with the longer axial lengths (≥28.00 mm in the both eyes), no new significant differences were found for rs2075555 and rs2269336 in our own study (data not shown). The summary OR for the meta-analysis using the subset was 1.27 (95% CI, 1.08–1.48; $P = 0.0035$) for rs2075555 and 1.25 (95% CI, 1.07–1.46; $P = 0.0051$) for rs2269336, respectively.

We also performed a systematic tSNP approach to assess the possible association between the *COL1A1* and high myopia in Japanese. The distributions of the allelic frequencies for all the eight tSNPs are given in Table 3. None of the eight tSNPs showed significant differences between the cases with high myopia and the control subjects with regard to the distribution of the genotype and allelic frequency. We also performed a

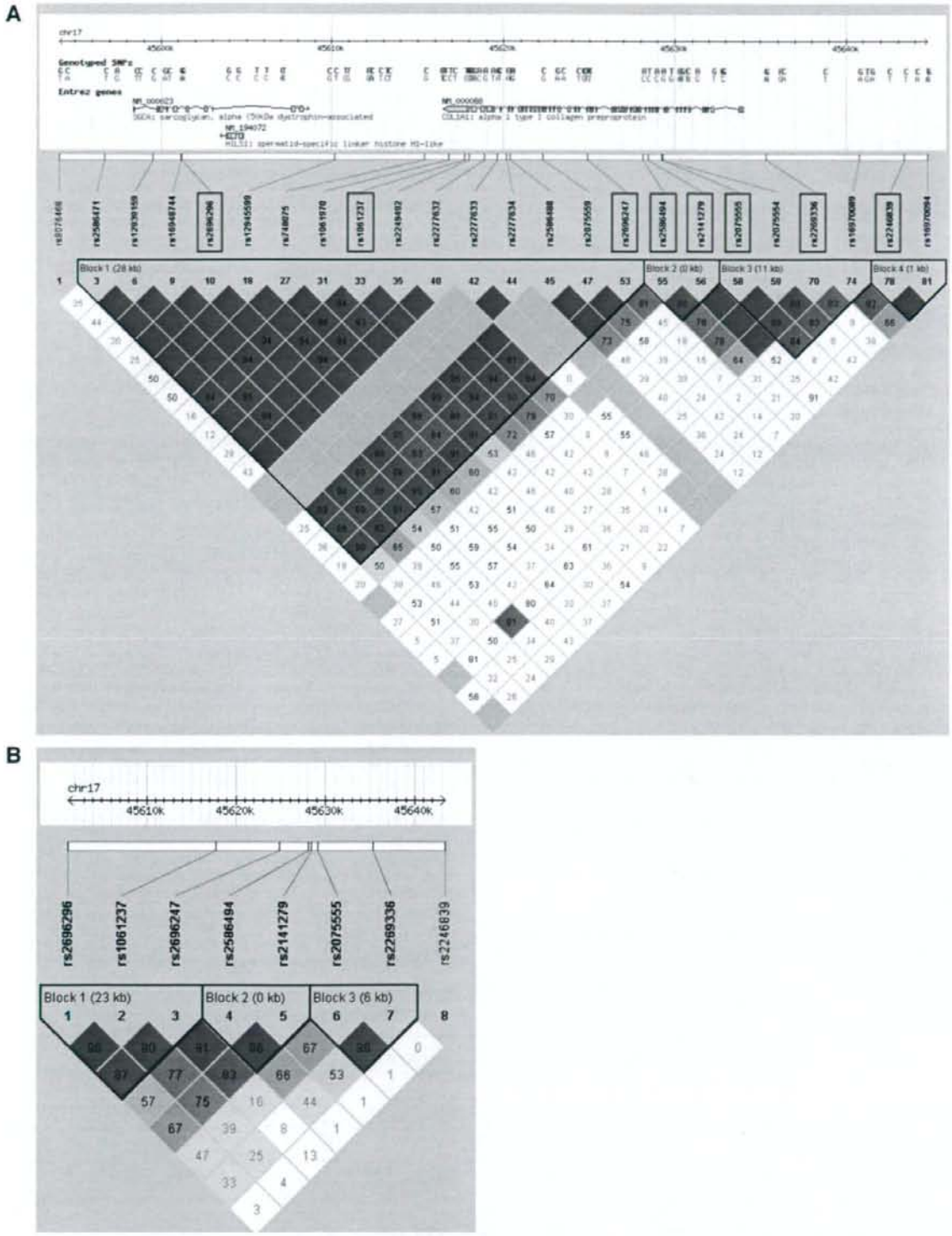

FIGURE 1. LD structure across the *COL1A1* region and selected tag SNPs. LD blocks were inferred by a solid spine of LD with a minimum D' of 0.8. **(A)** LD structure in Japanese samples from the HapMap database. SNPs with MAF > 5% are displayed, with the selected 8 tSNPs shown in boxes. **(B)** LD structure for the samples obtained in the present study (427 unrelated Japanese cases with high myopia [axial length ≥ 26.50 mm in both eyes] and 420 healthy Japanese controls). Three haplotype blocks were identified. The distribution of the haplotypes from each of the three blocks is shown in Table 4.

TABLE 1. Frequencies of Genotypes and Alleles of rs2075555 and rs2269336 in the Current Study

	Genotype					Allele				
SNP ID*		Case (%)	Control (%)	P†	OR (95% CI)		Case (%)	Control (%)	P†	OR (95% CI)
rs2075555	CC	167 (39.2)	158 (37.7)	0.736	1.17 (0.79–1.75)	C	528 (62.0)	505 (60.3)	0.471	1.07 (0.88–1.31)
	CA	194 (45.5)	189 (45.1)		1.14 (0.77–1.68)	A	324 (38.0)	333 (39.7)		
	AA	65 (15.3)	72 (17.2)		1.00 (ref.)					
rs2269336	CC	141 (33.8)	125 (29.9)	0.444	1.14 (0.78–1.67)	C	469 (56.2)	453 (54.2)	0.400	1.09 (0.90–1.32)
	CG	187 (44.8)	203 (48.6)		0.93 (0.65–1.33)	G	365 (43.8)	383 (45.8)		
	GG	89 (21.3)	90 (21.5)		1.00 (ref.)					

The nucleotides were defined on the forward strand of the reference sequence by dbSNP Build 126.

* SNP ID in National Center for Biotechnology Information (NCBI; Bethesda, MD) dbSNP Build 126.

† The nominal probabilities were calculated by the χ^2 test.

subset analysis on cases with axial lengths ≥ 28.00 mm. However, no new significant differences were found for the subjects in our study (data not shown).

We identified three haplotype blocks in the *COL1A1* gene (Fig. 1B). The estimated haplotype frequencies in the cases with high myopia and the control subjects are shown in Table 4. The haplotype frequencies were not significantly different between the patients with high myopia and the control subjects after the multiple testing corrections. Before correction, only one haplotype in block 1 showed a trend for a mildly significant difference in distribution ($P = 0.014$, $P_c = 0.14$). However, a haplotype analysis using the subset with axial lengths ≥ 28.00 mm did not show significant results for any of the blocks, even before correction (data not shown).

In addition, to check the results of our analyses using the same inclusion criteria that were used in a previous Japanese study,[36] we performed another subset analysis on 261 binocular phakic cases with refractions < −9.25 D (mean refraction ± SD, −14.46 ± 3.94 D; mean axial length ± SD, 29.17 ± 1.60 mm). The allelic frequency distributions for all the eight tSNPs in the subset analysis are given in Table 5. No new significant differences were noted for the genotype and allelic frequencies for rs2075555 and rs2269336. A haplotype in block 1 (the same haplotype described above) showed a trend for a mildly significant different distribution ($P = 0.034$, $P_c = 0.33$). However, there were no tSNPs or haplotypes that showed any significant differences after the multiple testing corrections.

DISCUSSION

The results in this study did not show significant associations with high myopia of the two SNPs of the *COL1A1* gene (rs2075555 and rs2269336, which have been reported to be high-myopia-susceptible SNPs in the Japanese population[36]). A systematic examination using the tSNP approach to access the possible association between the *COL1A1* gene and Japanese high myopia also did not find any significant results. The power calculation results that were based on the multiplicative model showed that our own observations rejected the reported ORs of rs2075555 (OR, 1.36) and rs2269336 (OR, 1.31) from the previous Japanese study with 85.9% and 78.7% power, respectively.

In our study, we defined high myopia by axial length instead of refraction. On the other hand, in the previous Japanese study that was included in our current analyses, they defined high myopia as refraction < −9.25 D.[36] Thus, one possible explanation for the discrepancy that was observed between the previous Japanese study and our own observations might be related to the difference in the way that high myopia was defined. To further examine this possibility, we performed a subset analysis on binocular phakic cases that had refraction < −9.25 D in both eyes, and we found no further significant differences in the present study. High myopia is most commonly defined by refraction. However, corneal curvature and the intraocular lens may also affect the refraction. Among these multiple factors, the axial length is the most important contributor to myopic refraction.[1–3] Hence, we suggest that the axial length is a more appropriate parameter than refraction when assessing the association between the *COL1A1* gene and high myopia. However, our study could not show any significant result whether the axial length or the refraction was chosen as the parameter. We cannot conclude which of the two, axial length or refraction, is the more appropriate parameter to assess the association between the *COL1A1* gene and high myopia.

TABLE 2. Meta-analysis* of the *COL1A1* rs2075555 and rs2269336 in Japanese Subjects with High Myopia

		Case		Control			
SNP ID†	Source	Subject Number	Risk Allele‡ *n* (%)	Subjects (*n*)	Risk Allele‡ *n* (%)	OR (95% CI)	P§
rs2075555	Current study	426	528 (62.0)	419	505 (60.3)	1.07 (0.88–1.31)	0.47
	Inamori et al.[36]	328	422 (64.3)	326	372 (57.1)	1.36 (1.09–1.70)	0.0071
	Total	754		745		1.19 (1.03–1.38)	0.022
rs2269336	Current study	417	469 (56.2)	418	453 (54.2)	1.09 (0.90–1.32)	0.40
	Inamori et al.[36]	329	397 (60.3)	330	354 (53.6)	1.31 (1.06–1.64)	0.014
	Total	746		748		1.18 (1.02–1.36)	0.026

* This meta-analysis was performed using the Mantel-Haenszel method based on the fixed-effect model.

† SNP ID in NCBI dbSNP Build 126.

‡ Risk alleles of rs2075555 (A/C) and rs2269336 (C/G) are allele C and allele C, respectively. The nucleotides were defined on the forward strand of the reference sequence by the dbSNP Build 126. We confirmed through personal communication that the nucleotides for rs2269336 (C/G) in a previous study by Inamori et al.[36] were defined on the reverse strand of the reference sequence by dbSNP.

§ The nominal probabilities were calculated by the χ^2 test.

TABLE 3. Association of Eight Tagged SNPs of the *COL1A1* with High Myopia in the Current Study

SNP ID*	Position†	Ref‡	Var‡	Case–Control		OR (95% CI)	P§	
				Allele Counts	Allele Frequencies		Nominal	Corrected
rs2696296	45601230	G	A	427:421, 395:445	0.504, 0.470	1.14 (0.94–1.38)	0.171	0.886
rs1061237	45617774	T	C	469:377, 477:339	0.554, 0.585	0.88 (0.73–1.07)	0.214	0.933
rs2696247	45624902	A	G	589:257, 567:271	0.696, 0.677	1.10 (0.89–1.35)	0.386	0.997
rs2586494	45628154	A	C	407:441, 425:409	0.480, 0.510	0.89 (0.73–1.08)	0.224	0.940
rs2141279	45628463	T	C	270:574, 268:568	0.320, 0.321	1.00 (0.81–1.22)	0.977	1.000
rs2075555	45629290	A	C	324:528, 333:505	0.380, 0.397	0.93 (0.77–1.13)	0.471	1.000
rs2269336	45635355	C	G	469:365, 453:383	0.562, 0.542	1.09 (0.90–1.32)	0.400	0.998
rs2246839	45643395	C	T	321:527, 321:511	0.379, 0.386	0.97 (0.80–1.18)	0.759	1.000

Axial length ≥ 26.5 mm in both eyes.

* SNP ID in NCBI dbSNP Build 126.

† Position of the polymorphism in the reference sequence NT_010783.14.

‡ Ref and Var were the reference and variant nucleotides, respectively, that were defined on the forward strand of the reference sequence by dbSNP.

§ The nominal probabilities were calculated by the χ^2 test, and the multiple testing corrections were performed by the permutation test (number of iterations = 10,000).

Another difference between the previous study and our own observations is that we used a population-based control. The prevalence of high myopia in the general population has been estimated to be approximately 1% to 5% in elderly adults.[2,11–16] Even if the control subjects in our study had no history of ocular diseases, the possibility exists that some of the eyes might have had an axial length ≥ 26.50 mm without the presence of vision threatening complications. If this were the case, this would be a possible explanation for the negative results that we found for our case-control association study. To check the results for a different axial-length-based definition, we also performed a subset analysis on cases with longer axial lengths (≥28.00 mm in both of the eyes). However, no new significant differences were found in the present study. Further subset analyses by redefining the cutoff value of axial length (27.00, 27.50, 28.50, and 29.00 mm) did not show any significant results (data not shown). Thus, we can conclude that the results of the present study did not replicate the previously reported Japanese study, which found significant associations for rs2075555 and rs2269336 with high myopia.

The results of our meta-analysis suggested that there were mildly significant associations between these two SNPs and high myopia in the Japanese population. However, it should be noted that we combined the data of our own study with the data of a previous Japanese study, a study that was the first to report positive results.[56] There was a potential for publication bias in the first positive study, and indeed, the reported ORs in the first positive studies were higher than most of the results that have been reported for subsequent replication studies.[58] Therefore, actual ORs of these SNPs are estimated at up to the ORs that are suggested by the results of the meta-analysis in this study. We concluded that the genetic risk in the *COL1A1* gene, if any, is weaker than has been originally reported.

In conclusion, the present study failed to replicate the positive association between the polymorphisms of the *COL1A1* gene and high myopia that has been reported in a prior study involving Japanese subjects. To elucidate whether the *COL1A1* gene in the MYP5 locus is associated with high myopia in the Japanese population, additional genetic and molecular biological studies are needed.

TABLE 4. Association of Haplotypes across the *COL1A1* Region with High Myopia in the Current Study

Haplotype*	Frequency	Case–Control		OR (95% CI)	P†	
		Ratio Counts	Frequencies		Nominal	Corrected
Block 1						
ATA	0.489	403.5:450.5, 424.3:415.7	0.472, 0.505	0.88 (0.73–1.06)	0.179	0.889
GCG	0.293	243.0:611.0, 253.0:587.0	0.285, 0.301	0.92 (0.75–1.14)	0.452	0.998
GCA	0.132	130.0:724.0, 93.7:746.3	0.152, 0.112	1.43 (1.08–1.90)	0.014	0.142
GTA	0.062	57.3:796.7, 48.3:791.7	0.067, 0.057	1.18 (0.79–1.75)	0.411	0.997
ATG	0.017	11.8:842.2, 17.3:822.7	0.014, 0.021	0.67 (0.32–1.41)	0.288	0.980
Block 2						
AC	0.488	405.6:448.4, 420.6:419.4	0.475, 0.501	0.90 (0.75–1.09)	0.289	0.980
CT	0.315	269.6:584.4, 263.3:576.7	0.316, 0.313	1.01 (0.82–1.24)	0.922	1.000
CC	0.192	175.9:678.1, 150.2:689.8	0.206, 0.179	1.19 (0.94–1.52)	0.156	0.842
Block 3						
CC	0.545	474.3:379.7, 448.3:391.7	0.555, 0.534	1.09 (0.90–1.32)	0.369	0.993
AG	0.381	319.3:534.7, 326.4:513.6	0.374, 0.389	0.94 (0.77–1.14)	0.533	0.999
CG	0.067	54.8:799.2, 57.9:782.1	0.064, 0.069	0.93 (0.63–1.36)	0.699	1.000

Axial length ≥ 26.5 mm in both eyes. The nucleotides were defined on the forward strand of the reference sequence by dbSNP Build 126.

* Haplotypes and linkage disequilibrium (LD) blocks were inferred by a solid spine of LD with a minimum D' of 0.8. The LD structure for the Japanese samples in the current study is shown in Figure 1(B).

† The nominal probabilities were calculated by the χ^2 test, with the multiple testing corrections performed by the permutation test (no. of iterations = 10,000).

TABLE 5. Association of Eight Tagged SNPs of *COL1A1* with a Subset of High Myopia in the Current Study

				Case–Control			*P*§	
SNP ID*	Position†	Ref‡	Var‡	Allele Frequencies	Allele Counts	OR (95% CI)	Nominal	Corrected
rs2696296	45601230	G	A	266:250, 395:445	0.516, 0.470	1.20 (0.96–1.49)	0.105	0.743
rs1061237	45617774	T	C	277:239, 477:339	0.537, 0.585	0.82 (0.66–1.03)	0.087	0.640
rs2696247	45624902	A	G	348:168, 567:271	0.674, 0.677	0.99 (0.78–1.25)	0.933	1.000
rs2586494	45628154	A	C	259:259, 425:409	0.500, 0.510	0.96 (0.77–1.20)	0.732	1.000
rs2141279	45628463	T	C	158:358, 268:568	0.306, 0.321	0.94 (0.74–1.19)	0.581	1.000
rs2075555	45629290	A	C	197:323, 333:505	0.379, 0.397	0.92 (0.74–1.16)	0.496	1.000
rs2269336	45635355	C	G	296:218, 453:383	0.576, 0.542	1.15 (0.92–1.43)	0.222	0.956
rs2246839	45643395	C	T	197:323, 321:511	0.379, 0.386	0.97 (0.77–1.22)	0.798	1.000

Eyes were binocular phakic and had refraction < −9.25 D.

* SNP ID in NCBI dbSNP Build 126.

† Position of the polymorphism in the reference sequence NT_010783.14.

‡ Ref and Var are, respectively, reference and variant nucleotides defined on the forward strand of the reference sequence by dbSNP.

§ The nominal probabilities were calculated by the χ^2 test, and the multiple testing corrections were performed by the permutation test (number of iterations = 10,000).

Acknowledgments

The authors thank Yasuo Kurimoto for assistance in recruiting the patients.

References

1. Wong TY, Foster PJ, Ng TP, Tielsch JM, Johnson GJ, Seah SK. Variations in ocular biometry in an adult Chinese population in Singapore: the Tanjong Pagar Survey. *Invest Ophthalmol Vis Sci.* 2001;42:73–80.
2. Wickremasinghe S, Foster PJ, Uranchimeg D, et al. Ocular biometry and refraction in Mongolian adults. *Invest Ophthalmol Vis Sci.* 2004;45:776–783.
3. Shufelt C, Fraser-Bell S, Ying-Lai M, Torres M, Varma R. Refractive error, ocular biometry, and lens opalescence in an adult population: the Los Angeles Latino Eye Study. *Invest Ophthalmol Vis Sci.* 2005;46:4450–4460.
4. Saw SM, Gazzard G, Shih-Yen EC, Chua WH. Myopia and associated pathological complications. *Ophthalmic Physiol Opt.* 2005;25:381–391.
5. Klaver CC, Wolfs RC, Vingerling JR, Hofman A, de Jong PT. Age-specific prevalence and causes of blindness and visual impairment in an older population: the Rotterdam Study. *Arch Ophthalmol.* 1998;116:653–658.
6. Buch H, Vinding T, La Cour M, Appleyard M, Jensen GB, Nielsen NV. Prevalence and causes of visual impairment and blindness among 9980 Scandinavian adults: the Copenhagen City Eye Study. *Ophthalmology.* 2004;111:53–61.
7. Evans JR, Fletcher AE, Wormald RP. Causes of visual impairment in people aged 75 years and older in Britain: an add-on study to the MRC Trial of Assessment and Management of Older People in the Community. *Br J Ophthalmol.* 2004;88:365–370.
8. Hsu WM, Cheng CY, Liu JH, Tsai SY, Chou P. Prevalence and causes of visual impairment in an elderly Chinese population in Taiwan: the Shihpai Eye Study. *Ophthalmology.* 2004;111:62–69.
9. Iwase A, Araie M, Tomidokoro A, Yamamoto T, Shimizu H, Kitazawa Y. Prevalence and causes of low vision and blindness in a Japanese adult population: the Tajimi Study. *Ophthalmology.* 2006;113:1354–1362.
10. Xu L, Wang Y, Li Y, et al. Causes of blindness and visual impairment in urban and rural areas in Beijing: the Beijing Eye Study. *Ophthalmology.* 2006;113:1134 e1–11.
11. Cheng CY, Hsu WM, Liu JH, Tsai SY, Chou P. Refractive errors in an elderly Chinese population in Taiwan: the Shihpai Eye Study. *Invest Ophthalmol Vis Sci.* 2003;44:4630–4638.
12. Shimizu N, Nomura H, Ando F, Niino N, Miyake Y, Shimokata H. Refractive errors and factors associated with myopia in an adult Japanese population. *Jpn J Ophthalmol.* 2003;47:6–12.
13. Bourne RR, Dineen BP, Ali SM, Noorul Huq DM, Johnson GJ. Prevalence of refractive error in Bangladeshi adults: results of the National Blindness and Low Vision Survey of Bangladesh. *Ophthalmology.* 2004;111:1150–1160.
14. Kempen JH, Mitchell P, Lee KE, et al. The prevalence of refractive errors among adults in the United States: Western Europe, and Australia. *Arch Ophthalmol.* 2004;122:495–505.
15. Hyman L. Myopic and hyperopic refractive error in adults: an overview. *Ophthalmic Epidemiol.* 2007;14:192–197.
16. Sawada A, Tomidokoro A, Araie M, Iwase A, Yamamoto T. Refractive errors in an elderly Japanese population: the Tajimi study. *Ophthalmology.* 2008;115:363–370 e3.
17. Saw SM, Katz J, Schein OD, Chew SJ, Chan TK. Epidemiology of myopia. *Epidemiol Rev.* 1996;18:175–187.
18. Kleinstein RN, Jones LA, Hullett S, et al. Refractive error and ethnicity in children. *Arch Ophthalmol.* 2003;121:1141–1147.
19. Ip JM, Huynh SC, Robaei D, et al. Ethnic differences in refraction and ocular biometry in a population-based sample of 11–15-year-old Australian children. *Eye.* 2008;22:649–656.
20. Klein AP, Duggal P, Lee KE, Klein R, Bailey-Wilson JE, Klein BE. Support for polygenic influences on ocular refractive error. *Invest Ophthalmol Vis Sci.* 2005;46:442–446.
21. Morgan IG. The biological basis of myopic refractive error. *Clin Exp Optom.* 2003;86:276–288.
22. Young TL, Metlapally R, Shay AE. Complex trait genetics of refractive error. *Arch Ophthalmol.* 2007;125:38–48.
23. Hammond CJ, Snieder H, Gilbert CE, Spector TD. Genes and environment in refractive error: the twin eye study. *Invest Ophthalmol Vis Sci.* 2001;42:1232–1236.
24. Lyhne N, Sjolie AK, Kyvik KO, Green A. The importance of genes and environment for ocular refraction and its determiners: a population based study among 20–45 year old twins. *Br J Ophthalmol.* 2001;85:1470–1476.
25. Hammond CJ, Andrew T, Mak YT, Spector TD. A susceptibility locus for myopia in the normal population is linked to the PAX6 gene region on chromosome 11: a genomewide scan of dizygotic twins. *Am J Hum Genet.* 2004;75:294–304.
26. Dirani M, Chamberlain M, Garoufalis P, Chen C, Guymer RH, Baird PN. Refractive errors in twin studies. *Twin Res Hum Genet.* 2006;9:566–572.
27. Dirani M, Chamberlain M, Shekar SN, et al. Heritability of refractive error and ocular biometrics: the Genes in Myopia (GEM) twin study. *Invest Ophthalmol Vis Sci.* 2006;47:4756–4761.
28. Zhu G, Hewitt AW, Ruddle JB, et al. Genetic Dissection of myopia evidence for linkage of ocular axial length to chromosome 5q. *Ophthalmology.* 2008;115:1053–1057.e2.
29. Jacobi FK, Zrenner E, Broghammer M, Pusch CM. A genetic perspective on myopia. *Cell Mol Life Sci.* 2005;62:800–808.
30. Tang WC, Yap MK, Yip SP. A review of current approaches to identifying human genes involved in myopia. *Clin Exp Optom.* 2008;91:4–22.